Sliced Optimal Partial Transport

Yikun Bai*¹, Bernard Schmitzer*², Mathew Thorpe^{3,4}, and Soheil Kolouri¹

¹Department of Computer Science, Vanderbilt University
²Institute of Computer Science, Göttingen University
³Department of Mathematics, University of Manchester
⁴The Alan Turing Institute
¹yikun.bai,soheil.kolouri@vanderbilt.edu
²schmitzer@cs.uni-goettingen.de
³matthew.thorpe-2@manchester.ac.uk

Abstract

Optimal transport (OT) has become exceedingly popular in machine learning, data science, and computer vision. The core assumption in the OT problem is the equal total amount of mass in source and target measures, which limits its application. Optimal Partial Transport (OPT) is a recently proposed solution to this limitation. Similar to the OT problem, the computation of OPT relies on solving a linear programming problem (often in high dimensions), which can become computationally prohibitive. In this paper, we propose an efficient algorithm for calculating the OPT problem between two non-negative measures in one dimension. Next, following the idea of sliced OT distances, we utilize slicing to define the sliced OPT distance. Finally, we demonstrate the computational and accuracy benefits of the sliced OPT-based method in various numerical experiments. In particular, we show an application of our proposed Sliced-OPT in noisy point cloud registration.

1 Introduction

The Optimal Transport (OT) problem studies how to find the most cost-efficient way to transport one probability measure to another, and it gives rise to popular probability metrics like the Wasserstein distance. OT has attracted abundant attention in data science, statistics, machine learning, signal processing and computer vision [50, 23, 40, 32, 1, 25, 38, 52, 14, 13].

A core assumption in the OT problem is the equal total amount of mass in the source and target measures (e.g., probability measures). Many practical problems, however, deal with comparing non-negative measures with varying total amounts of mass, e.g., shape analysis [49, 10], domain adaptation [18], color transfer [11]. In addition, OT distances are often not robust to outliers and noise, as transporting outliers could be prohibitively expensive and might compromise the distance estimation. To address these issues, many variants of the OT problem have been recently proposed, for example, the optimal partial transport (OPT) problem [7, 20, 21], the Hellinger–Kantorovich distance [10, 37], and Kantorovich–Rubinstein norm [26, 36]. These variants were subsequently unified under the name "unbalanced optimal transport" [12, 37].

The computational complexity of linear programming for balanced and partial OT problems is often a bottleneck for solving large-scale problems. Different approaches have been developed to address this issue. For instance, by entropic regularization, the problem becomes strictly convex and can be solved with the celebrated Sinkhorn–Knopp algorithm [15, 48] which has been extended to the unbalanced setting [11]. This approach can still be computationally expensive for small regularization levels. Other strategies exploit specific properties of ground costs. For example, if the ground cost is determined by the unique path on a tree, the problem can be efficiently solved in the balanced [42, 34] and the unbalanced setting [47]. In particular,

^{*}These authors contributed equally to this work.

balanced 1-dimensional transport problems with convex ground costs can be solved by the north-west corner rule, which essentially amounts to sorting the support points of the two input measures.

Based on this, another popular method is the sliced OT approach [45, 31, 5], which assumes the ground cost is consistent with the Euclidean distance (in 1-dimensional space). Furthermore, it has been shown [31, 33, 47] that the OT distance in Euclidean space can be approximated by the OT distance in 1-dimensional Euclidean space. Inspired by these works, in this paper, we propose the sliced version of OPT and an efficient computational algorithm for empirical distributions with uniform weights, i.e., measures of the form $\sum_{i=1}^{n} \delta_{x_i}$, where δ_x is the Dirac measure. Our contributions in this paper can be summarized as follows:

- We propose a primal-dual algorithm for 1-dimensional OPT with a quadratic worst-case time complexity and super linear complexity in practice.
- In d-dimensional space, we propose the Sliced-OPT (SOPT) distance. Similar to the sliced OT distance, we prove that it satisfies the metric axioms and propose a computational method based on our 1-dimensional OPT problem solver.
- We demonstrate an application of SOPT in point cloud registration by proposing a SOPT variant of the *iterative closest point* (ICP) algorithm. Our approach is robust against noise. Also, we apply SOPT to a color adaptation problem.

2 Related Work

Linear programming. In the discrete case, the Kantorovich formulation [28] of OT problem is a (high-dimensional) linear program [29]. As shown in [7], OPT can be formulated as a balanced OT problem by introducing *reservoir* points, thus it could also be solved by linear programming. However, the time complexity is prohibitive for large datasets.

Entropy Regularization. Entropic regularization approaches add the transport plan's entropy to the OT objective function and then apply the Sinkhorn-Knopp algorithm [48, 15]. The algorithm can be extended to the large-scale stochastic [24] and unbalanced setting [2, 11]. For moderate regularization these algorithms converge fast, however, there is a trade-off between accuracy versus stability and convergence speed for small regularization.

Sliced OT. Sliced OT techniques [45, 31, 5, 39, 33] rely on the closed-form solution for the balanced OT map in 1-dimensional Euclidean settings, i.e., the increasing re-arrangement function given by the northwest corner rule. The main idea behind these methods is to calculate the expected OT distance between the 1-dimensional marginal distributions (i.e., slices) of two d-dimensional distributions. The expectation is numerically approximated via a Monte Carlo integration scheme. Other extensions of these distances include the generalized and the max-sliced Wasserstein distances [30, 16]. In the unbalanced setting, and for a particular case of OPT, [4] propose a fast (primal) algorithm, which has quadratic worst-case time complexity, and often linear complexity in practice. In particular, Bonneel et al. [4] assume that all the mass in the source measure must be transported to the target measure, i.e., no mass destruction happens in the source measure.

Other computational methods. When the transportation cost is a metric, network flow methods [26, 41] can be applied. For metrics on trees, an efficient algorithm based on dynamic programming with time complexity $\mathcal{O}(n\log^2 n)$ is proposed in [47]. However, in high dimensions existence (and identification) of an appropriate metric tree remains challenging.

3 Background of Optimal (Partial) Transport

We first review the preliminary concepts of the OT and the OPT problems. In what follows, given $\Omega \subset \mathbb{R}^r$, $p \geq 1$, we denote by $\mathcal{P}(\Omega)$ the set of Borel probability measures and by $\mathcal{P}_p(\Omega)$ the set of probability measures with finite p'th moment defined on a metric space (Ω, d) .

Optimal transport. Given $\mu, \nu \in \mathcal{P}(\Omega)$, and a lower semi-continuous function $c: \Omega^2 \to \mathbb{R}_+$, the OT problem between μ and ν in the *Kantorovich formulation* [28], is defined as:

$$OT(\mu, \nu) := \inf_{\gamma \in \Gamma(\mu, \nu)} \int_{\Omega^2} c(x, y) \, d\gamma(x, y), \tag{1}$$

where $\Gamma(\mu,\nu)$ is the set of all joint probability measures whose marginal are μ and ν . Mathematically, we denote as $\pi_{1\#}\gamma = \mu$, $\pi_{2\#}\gamma = \nu$, where π_1, π_2 are canonical projection maps, and for any (measurable) function $f:\Omega^2 \to \Omega$, $f_{\#}\gamma$ is the push-forward measure defined as $f_{\#}\gamma(A) = \gamma(f^{-1}(A))$ for any Borel set $A \subset \Omega$. When c(x,y) is a p-th power of a metric, the p-th root of the induced optimal value is the **Wasserstein distance**, a metric in $\mathcal{P}_p(\Omega)$.

Optimal Partial Transport. The OPT problem, in addition to mass transportation, allows mass destruction on the source and mass creation on the target. Here the mass destruction and creation penalty will be linear. Let $\mathcal{M}_+(\Omega)$ denote the set of all positive Radon measures defined on Ω , suppose $\mu, \nu \in \mathcal{M}_+(\Omega)$, and $\lambda_1, \lambda_2 \geq 0$, the OPT problem is:

$$OPT_{\lambda_1,\lambda_2}(\mu,\nu) := \inf_{\substack{\gamma \in \mathcal{M}_+(\Omega^2) \\ \pi_1 \# \gamma \le \mu, \pi_2 \# \gamma \le \nu}} \int c(x,y) \, \mathrm{d}\gamma + \lambda_1(\mu(\Omega) - \pi_1 \# \gamma(\Omega)) + \lambda_2(\nu(\Omega) - \pi_2 \# \gamma(\Omega)) \tag{2}$$

where the notation $\pi_{1\#}\gamma \leq \mu$ denotes that for any Borel set $A \subseteq \Omega$, $\pi_{1\#}\gamma(A) \leq \mu(A)$, and we say $\pi_{1\#}\gamma$ is dominated by μ , analogously for $\pi_{2\#}\gamma \leq \nu$; the notation $\mu(\Omega)$ denotes the total mass of measure μ . We denote the set of such γ by $\Gamma_{\leq}(\mu,\nu)$. When the transportation cost c(x,y) is a metric, and $\lambda_1 = \lambda_2$, OPT(\cdot,\cdot) defines a metric on $\mathcal{M}_{+}(\Omega)$ (see [12, Proposition 2.10], [43, Proposition 5], [35, Section 2.1] and [8, Theorem 4]). For finite λ_1 and λ_2 let $\lambda = \frac{\lambda_1 + \lambda_2}{2}$ and define:

$$\begin{aligned}
OPT_{\lambda}(\mu,\nu) &:= OPT_{\lambda,\lambda}(\mu,\nu) \\
&= OPT_{\lambda_{1},\lambda_{2}}(\mu,\nu) - K_{\lambda_{1},\lambda_{2}}(\mu,\nu)
\end{aligned} (3)$$

where,

$$K_{\lambda_1,\lambda_2}(\mu,\nu) = \frac{\lambda_1 - \lambda_2}{2}\mu(\Omega) + \frac{\lambda_2 - \lambda_1}{2}\nu(\Omega).$$

Since for fixed μ and ν , K_{λ_1,λ_2} is a constant, and without the loss of generality, in the rest of the paper, we only consider $\text{OPT}_{\lambda}(\mu,\nu)$. The case where λ_i s are not finite is discussed in Section 4.1.

Various equivalent formulations of OPT (3) have appeared in prior work, e.g., [21, 20, 43], which were later unified as a special case of unbalanced OT [12, 37]. We provide a short summary of these formulations and their relationship with unbalanced OT in the appendix. OPT has several desirable theoretical properties. For instance, by [43, Proposition 5], minimizing γ exist and they are concentrated on c-cyclical monotone sets. More concretely, we have the following proposition.

Proposition 3.1. Let γ^* be a minimizer in (3), then the support of γ^* satisfies the c-cyclical monotonicity property: for any $n \in \mathbb{N}$, any $\{(x_i, y_i)\}_{i=1}^n \subset \operatorname{supp}(\gamma^*)$ and any permutation $\sigma : [1:n] \to [1:n]$ we have

$$\sum_{i=1}^{n} c(x_i, y_i) \le \sum_{i=1}^{n} c(x_i, y_{\sigma(i)}).$$

In particular, in one dimension, for c(x,y) = f(|x-y|) where $f: \mathbb{R} \to \mathbb{R}_+$ is a convex increasing function, c-cyclical monotonicity is equivalent to

$$(x_1, y_1), (x_2, y_2) \in \text{supp}(\gamma^*)$$
 \Rightarrow $[x_1 \le x_2 \text{ and } y_1 \le y_2] \text{ or } [x_1 \ge x_2 \text{ and } y_1 \ge y_2].$

Proof. Let $\hat{\gamma}$ be optimal for the extended balanced problem of appendix section B, (11), and let γ be the restriction of this measure to $\Omega \times \Omega$. Since restriction preserves optimality [54, Theorem 4.6], γ must be an optimal plan between $\pi_{1\#}\gamma$ and $\pi_{2\#}\gamma$ with respect to the (non-extended) cost c on $\Omega \times \Omega$. Therefore, it must be supported on a c-cyclically monotone set [54, Theorem 5.10]. In one dimension, for costs of the form c(x,y)=f(x-y) for convex f, c-cyclical monotonicity reduces to standard monotonicity, see for instance [46, Theorem 2.9].

To further simplify (3), we show in the following lemma that the support of the optimal γ does not contain pairs of (x, y) whose cost exceeds 2λ .

Lemma 3.2. There exists an optimal γ^* for (3) such that $\gamma^*(S) = 0$, where $S = \{(x, y) \in \Omega^2 : c(x, y) \ge 2\lambda\}$.

Proof. Pick γ and define γ' as follows: for any Borel $A \subset \Omega^2$, $\gamma'(A) = \gamma(A \setminus S)$. Let

$$C(\gamma) := \int c(x, y) \, d\gamma + \lambda \left[(\mu(\Omega) - \pi_{1\#}\gamma(\Omega)) + (\nu(\Omega) - \pi_{2\#}\gamma(\Omega)) \right]$$
$$= \int (c(x, y) - 2\lambda) \, d\gamma + \lambda (\mu(\Omega) + \nu(\Omega)),$$

which is the objective function for the OPT problem defined in (3), and the second line follows from the fact $\gamma(\Omega^2) = (\pi_1)_{\#}\gamma(\Omega) = (\pi_2)_{\#}\gamma(\Omega)$. Then we have

$$C(\gamma) - C(\gamma') = \int_{S} (c(x, y) - 2\lambda) \, d\gamma(x, y) \ge 0$$

That is, for any γ , we can find a better transportation plan γ' such that $\gamma'(S) = 0$.

4 Empirical Optimal Partial Transport

In \mathbb{R}^r , suppose μ, ν are n and m-size empirical distributions, i.e., $\mu = \sum_{i=1}^n \delta_{x_i}$ and $\nu = \sum_{j=1}^m \delta_{y_j}$. The OPT problem (3), denoted as OPT($\{x_i\}_{i=1}^n, \{y_j\}_{j=1}^m$) can be written as

$$OPT(\{x_i\}_{i=1}^n, \{y_j\}_{j=1}^m) := \min_{\gamma \in \Gamma_{\leq}(\mu, \nu)} \sum_{i,j} c(x_i, y_j) \gamma_{ij} + \lambda(n + m - 2\sum_{i,j} \gamma_{ij})$$
(4)

where

$$\Gamma_{\leq}(\mu,\nu) := \{ \gamma \in \mathbb{R}_+^{n \times m} : \gamma 1_m \leq 1_n, \gamma^T 1_n \leq 1_m \},^*$$

and 1_n denotes the $n \times 1$ vector whose entries are 1 and analogously for 1_m . We show that the optimal plan γ for the empirical OPT problem is induced by a 1-1 mapping. A similar result is known for continuous measures μ and ν , see [20, Proposition 2.4 and Theorem 2.6].

Theorem 4.1. There exists an optimal plan for $OPT(\{x_i\}_{i=1}^n, \{y_j\}_{j=1}^m)$, which is induced by a 1-1 mapping, i.e., $\gamma_{ij} \in \{0,1\}, \forall i,j$ and in each row and column, at most one entry of γ is 1.

Proof. We start by adapting the extension (11) to the concrete discrete setting between empirical measures. Let $\hat{\Omega} = [1:m+n]$, and let $\hat{c}: \hat{\Omega} \times \hat{\Omega}$ be given by

$$\hat{c}(i,j) = \begin{cases} c(x_i, y_j) - 2\lambda & \text{if } i \leq n, j \leq m, \\ 0 & \text{otherwise.} \end{cases}$$

Let $\hat{\mu} = \hat{\nu} = \sum_{i=1}^{m+n} \delta_i$. Then solving the (balanced) optimal transport problem on $\hat{\Omega}$ between $\hat{\mu}$ and $\hat{\nu}$ with respect to cost \hat{c} is (as above) clearly equivalent to the OPT problem, and an optimal OPT plan can be obtained by restricting an optimal $\hat{\gamma}$ to the set $[1:n] \times [1:m]$. Note that here we have simply split the mass on the isolated point $\hat{\infty}$ onto multiple points, where each only carries unit mass. At the same time, the set $\Gamma(\hat{\mu},\hat{\nu})$ are the doubly stochastic matrices and by the Birkhoff-von-Neumann theorem, its extremal points are permutation matrices. Thus there always exists an optimal $\hat{\gamma}$ that is a permutation matrix, and thus its restriction to $[1:n] \times [1:m]$ will only contain entries 0 or 1, with at most one 1 per row and column.

Combining this theorem and the cyclic monotonicity of 1D OPT, we can restrict the optimal mapping to strictly increasing maps.

^{*}Here the rigorous notation should be $\Pi_{<}(1_n,1_m)$. But we abuse the notation for convenience.

Corollary 4.2. For $\{x_i\}_{i=1}^n$, $\{y_j\}_{j=1}^m$ sorted point lists in \mathbb{R} , and a cost function c(x,y) = h(x-y) where $h: \mathbb{R} \to \mathbb{R}$ is strictly convex, the empirical OPT problem $OPT(\{x_i\}_{i=1}^n, \{y_j\}_{j=1}^m)$ can be further simplified to

$$OPT(\{x_i\}_{i=1}^n, \{y_j\}_{j=1}^m) := \min_{L} C(L)$$
(5)

where

$$C(L) := \sum_{i \in \text{dom}(L)} c(x_i, y_{L[i]}) + \lambda \left(n + m - 2 \left| \text{dom}(L) \right| \right),$$

 $and \ L:[1:n] \rightarrow \{-1\} \cup [1:m], \ dom(L):=\{i:L[i] \neq -1\}, \ L_{|dom(L)}:[1:n] \hookrightarrow [1:m] \ is \ a \ strictly \ increasing mapping.$

For convenience, we call any mapping $L:[1:n] \to \{-1\} \cup [1:m]$ a "transportation plan" (or "plan" for short). Furthermore, since L can be represented by a vector, we do not distinguish L(i), L[i], and L_i . Of course, there is a bijection between admissible L and γ and we use this equivalence implicitly in the following.

Importantly, the OPT problem is a convex optimization problem and therefore has a dual form which is given by the following proposition.

Proposition 4.3. The primal problem (4) admits the dual form

$$\sup_{\substack{\Phi \in \mathbb{R}^n, \Psi \in \mathbb{R}^m \\ \Phi_i + \Psi_j \leq c(x_i, y_j) \, \forall i, j}} \sum_{i=1}^n \min\{\Phi_i, \lambda\} + \sum_{j=1}^m \min\{\Psi_j, \lambda\}.$$

Moreover, the following are necessary and sufficient conditions for $\gamma \in \Gamma_{\leq}(\mu, \nu)$, $\Phi \in \mathbb{R}^n$ and $\Psi \in \mathbb{R}^m$ to be optimal for the primal and dual problems:

$$\begin{split} &\Phi_i + \Psi_j = c(x_i, y_j), \forall (x_i, y_j) \in \operatorname{supp}(\gamma) \\ &\Phi_i < \lambda \Rightarrow [\pi_{1\#}\gamma]_i = 1 \\ &\Phi_i = \lambda \Rightarrow [\pi_{1\#}\gamma]_i \in [0, 1] \\ &\Phi_i > \lambda \Rightarrow [\pi_{1\#}\gamma]_i = 0 \end{split} \qquad \begin{aligned} &\Psi_j < \lambda \Rightarrow [\pi_{2\#}\gamma]_j = 1 \\ &\Psi_j = \lambda \Rightarrow [\pi_{2\#}\gamma]_j \in [0, 1] \\ &\Psi_i > \lambda \Rightarrow [\pi_{2\#}\gamma]_j = 0. \end{aligned}$$

Proof. For $\lambda_1 = \lambda_2$ we can write (2) as

$$\mathrm{OPT}_{\lambda}(\mu,\nu) = \mathrm{ET}(\mu,\nu;\mathcal{F},\mathcal{F}) = \inf_{\gamma \geq 0} \int_{\Omega^2} c \mathrm{d}\gamma + \mathcal{F}(\pi_{1\#}\gamma \parallel \mu) + \mathcal{F}(\pi_{2\#}\gamma \parallel \nu)$$

where $\mathcal{F}(\hat{\mu} \parallel \mu)$ is called Csiszàr f-divergence, defined as

$$\mathcal{F}(\hat{\mu} \parallel \mu) := \int F(\sigma) d\mu + F_{\infty}' \gamma^{\perp}(\Omega) = \begin{cases} \lambda \cdot (\mu(\Omega) - \hat{\mu}(\Omega)) & \text{if } 0 \leq \hat{\mu} \leq \mu \\ +\infty & \text{otherwise} \end{cases},$$

with the integrand F

$$F(s) = \begin{cases} \lambda(1-s) & \text{if } s \in [0,1] \\ +\infty & \text{else} \end{cases},$$

and σ , μ^{\perp} is defined by Lebesgue's decomposition theorem $\mu = \frac{d\hat{\mu}}{d\mu} + \mu^{\perp}$; $F'_{\infty} := \lim_{s \to \infty} \frac{F(s)}{s}$ is called recession constant of F (We refer [37, section 2.1] for more details).

By [37, Theorem 4.11] the dual of ET is

$$\sup_{\substack{\Phi \in \mathrm{L}^1(\mu), \Psi \in \mathrm{L}^1(\nu) \\ \Phi \oplus \Psi \leq c \\ \Phi, \Psi \text{ lsc and bounded}}} - \int_{\Omega} F^*(-\Phi) \, \mathrm{d}\mu - \int_{\Omega} F^*(-\Psi) \, \mathrm{d}\nu$$

^{*}Here, mapping a point to $\{-1\}$ corresponds to destroying the point in the source, while unmatched points in the target are created. Hence, L uniquely represents the partial transport.

where $F^*: \mathbb{R} \to (-\infty, \infty]$, called Legendre conjugate function, is defined as

$$F^*(r) = \sup_{s} (rs - F(s)) = \max\{-\lambda, r\}.$$

By [37, Theorem 4.6] the optimality conditions are

$$\Phi \oplus \Psi = c \qquad \gamma\text{-a.e.}$$

$$-\Phi \in \partial F \left(\frac{d\gamma_1}{d\mu}\right), \quad \gamma_1 = \pi_{1\#}\gamma \qquad \mu\text{-a.e.}$$

$$-\Psi \in \partial F \left(\frac{d\gamma_2}{d\nu}\right), \quad \gamma_2 = \pi_{2\#}\gamma \qquad \nu\text{-a.e.}$$
(6)

We have

$$\partial F(s) = \begin{cases} \{-\lambda\} & \text{if } s \in (0,1) \\ (-\infty, -\lambda] & \text{if } s = 0 \\ [-\lambda, +\infty) & \text{if } s = 1. \end{cases}$$

So (6) can be written

$$\Phi(x) = \lambda \qquad \qquad \text{if } \frac{\mathrm{d}\gamma_1}{\mathrm{d}\mu}(x) \in (0,1)$$

$$\Phi(x) \in [\lambda, +\infty) \qquad \qquad \text{if } \frac{\mathrm{d}\gamma_1}{\mathrm{d}\mu}(x) = 0$$

$$\Phi(x) \in (-\infty, \lambda] \qquad \qquad \text{if } \frac{\mathrm{d}\gamma_1}{\mathrm{d}\mu}(x) = 1.$$

Similarly for Ψ . In the discrete case, the dual problem and optimality conditions reduce to the form stated in the proposition.

4.1 A Quadratic Time Algorithm

Our algorithm finds the solutions γ , Φ , and Ψ to the primal-dual optimality conditions given in Proposition 4.3. We assume that, at iteration k, we have solved $\mathrm{OPT}(\{x_i\}_{i=1}^{k-1}, \{y_j\}_{j=1}^m)$ in the previous iteration (stored in L[1:k-1]) and we now proceed to solve $\mathrm{OPT}(\{x_i\}_{i=1}^k, \{y_j\}_{j=1}^m)$ in the current iteration. Recall that we assume that $\{x_i\}_{i=1}^n$ and $\{y_j\}_{j=1}^m$ are sorted and that L[i] is the index determining the transport of mass from x_i , i.e., if $L[i] \neq -1$ then x_i is associated to $y_{L[i]}$. For simplicity we assume for now that all points in $\{x_i\}_{i=1}^n$ are distinct, and likewise for $\{y_j\}_{j=1}^m$. Duplicate points can be handled properly with some minor additional steps (see appendix). Let j^* be the index of the most attractive $\{y_j\}_{j=1}^m$ for the new point x_k under consideration of the dual variables, i.e., $j^* = \mathrm{argmin}_{j \in [1:m]} c(x_k, y_j) - \Psi_j$ and set $\Phi_k = \min\{c(x_k, y_{j^*}) - \Psi_{j^*}, \lambda\}$ so that Φ_k is the largest possible value satisfying the dual constraints, but no greater than λ since at this point the dual objective becomes flat. We now distinguish three cases:

Case 1: If $\Phi_k = \lambda$, then destroying x_k is the most efficient action, i.e., we set L[k] = -1 and proceed to k+1.

Case 2: If $\Phi_k < \lambda$ and y_{j^*} is unassigned, then we set $L[k] = j^*$ and we can proceed to k+1.

Case 3: If $\Phi_k < \lambda$ and y_{j^*} is already assigned, we must resolve the conflict between x_k and the element currently assigned to y_{j^*} . This will be done by a sub-algorithm.

It is easy to see that in the first two cases, if L (or γ), Φ and Ψ satisfy the primal-dual conditions of Proposition 4.3 up until k-1, they will now satisfy them up until k. Let us now study the third case in more detail.

One finds that if y_{j^*} is already assigned, then it must be to x_{k-1} (proof in appendix). We now increase Φ_i for $i \in [k-1:k]$ while decreasing Ψ_{j^*} (at the same rate) until one of the following cases occurs:

Case 3.1: Either Φ_{k-1} or Φ_k reaches λ . In this case, the corresponding x becomes unassigned and the other becomes (or remains) assigned to j^* . The conflict is resolved and we proceed to solve the problem for k+1.

- Case 3.2: One reaches the point where $\Phi_k + \Psi_{j^*+1} = c(x_k, y_{j^*+1})$. In this case, x_k becomes assigned to y_{j^*+1} , the conflict is resolved and we move to k+1.
- Case 3.3a: One reaches the point where $\Phi_{k-1} + \Psi_{j^*-1} = c(x_{k-1}, y_{j^*-1})$. If y_{j^*-1} is unassigned, we assign x_{k-1} to y_{j^*-1} , x_k to y_{j^*} . The conflict is resolved and we move on.
- Case 3.3b: In the remaining case where y_{j^*-1} is already assigned, we will show that it must be to x_{k-2} . This means that the set of points involved in the conflict increases and we must perform a slight generalization of the above case 3 iteration until eventually one of the other cases occurs.

At each iteration we consider a contiguous set of $\{x_i\}_{i=i_{\min}}^{k-1}$ assigned monotonously to contiguous $\{y_j\}_{j=j_{\min}}^{j^*}$, where i_{\min} is initially set $i_{\min} = k-1$ and j_{\min} is the index of y_j that has been assigned to $x_{i_{\min}}$ (i.e., $j_{\min} = j^*$), and the additional point x_k . We increase Φ_i for $i \in [i_{\min}:k]$ and decrease Ψ_j for $j \in [j_{\min}:j^*]$, until either $\Phi_{k'}$ becomes equal to λ for some $k' \in [i_{\min}:k+1]$ (Case 3.1), $\Phi_k + \Psi_{j^*+1} = c(x_k, y_{j^*+1})$ (Case 3.2) or $\Phi_{i_{\min}} + \Psi_{j_{\min}-1} = c(x_{i_{\min}}, y_{j_{\min}-1})$ (Case 3.3). In Cases 3.1 and 3.2 the conflict can be resolved in an obvious way. The same holds for Case 3.3, when $y_{j_{\min}-1}$ is unassigned (Case 3.3a). Otherwise (Case 3.3b), one adds one more assigned pair to the chain and restarts the loop with the pair $(x_{i_{\min}-1}, y_{j_{\min}-1})$ added to the chain. Of course, trivial adaptations have to be made to account for boundary effects, e.g., Case 3.2 cannot occur if $j^* = m$ etcetera. A pseudocode description of the method is given by Algorithms 1 and 2, and a visual illustration of these algorithms is provided in Figure 1. Note that for the sake of legibility, we make some simplifications, e.g., boundary checks are ignored (see above), and we do not specify how to keep track of whether j^* is assigned or not. Also, updating the dual variables at each iteration of the sub-routine yields a cubic worst-case time complexity, but is easier to understand. A complete version of the algorithm with all checks, appropriate data structures, and quadratic complexity is given in the appendix. There we also prove the following claim:

Theorem 4.4. Algorithm 1 is correct, i.e., it is well-defined and returns optimal primal and dual solutions L and (Φ, Ψ) to the 1-dimensional OPT problem for sorted $\{x_i\}_{i=1}^n$, $\{y_j\}_{j=1}^m$. A slight adaptation of the algorithm (given in the appendix) has a worst-case time complexity of $O(n \max\{m, n\})$.

The algorithm can be adjusted to the case where $\lambda_1 = \infty$ by setting all instances of λ in Algorithms 1 and 2 to $+\infty$ except for the initialization of Ψ . This means that cases 1 and 3.1 never occur. The algorithm then reduces to a primal-dual version of that given in [4]. If $\lambda_2 = \infty$, then one simply flips the two marginals and proceeds as for $\lambda_1 = \infty$.

```
Algorithm 1: opt-1d
```

```
Input: \{x_i\}_{i=1}^n, \{y_j\}_{j=1}^m, \lambda
    Output: L, \Psi, \Phi
 1 Initialize \Phi_i \leftarrow -\infty for i \in [1:n], \Psi_j \leftarrow \lambda for j \in [1:m] and L_i \leftarrow -1 for i \in [1:n]
 2 for k = 1, 2, ... n do
         j^* \leftarrow \operatorname{argmin}_{j \in [1:m]} c(x_k, y_j) - \Psi_j
         \Phi_k \leftarrow \min\{c(x_k, y_{j^*}) - \Psi_{j^*}, \lambda\}
 4
         if \Phi_k = \lambda then
 5
           [Case 1] No update on L
 6
         else if j^* unassigned then
 7
              [Case 2] L_k \leftarrow j^*
 8
 9
              [Case 3] Run Algorithm 2.
10
```

4.2 Runtime Analysis

We test the wall clock time by sampling the point lists from uniform distributions and Gaussian mixtures. In particular, we set $\{x_i\}_{i=1}^n \stackrel{\text{iid}}{\sim} \text{Unif}[-20,20], \{y_j\}_{j=1}^m \stackrel{\text{iid}}{\sim} \text{Unif}[-40,40], \lambda \in \{20,100\} \text{ and } \{x_i\}_{i=1}^n \stackrel{\text{iid}}{\sim} \text{Unif}[-40,40], \lambda \in \{20,100\}$

```
Algorithm 2: sub-opt
```

```
Input: (\{x_i\}_{i=1}^n, \{y_j\}_{j=1}^m, k, j^*, L, \Phi, \Psi)
     Output: (Updated L, \Phi, \Psi, optimal for \mathrm{OPT}(\{x_i\}_{i=1}^k, \{y_j\}_{j=1}^m))
 1 Initialize i_{\min} \leftarrow k - 1, j_{\min} \leftarrow j^*.
  2 while true do
            i_{\Delta} \leftarrow \operatorname{argmin}_{i \in [i_{\min}:k]}(\lambda - \Phi_i)
 3
            \lambda_{\Delta} \leftarrow \lambda - \Phi_{i_{\Delta}}
  4
            \alpha \leftarrow c(x_k, y_{j^*+1}) - \Phi_k - \Psi_{j^*+1}
  5
            \beta \leftarrow c(x_{i_{\min}}, y_{j_{\min}-1}) - \Phi_{i_{\min}} - \Psi_{j_{\min}-1}
  6
            if \lambda_{\Delta} \leq \min\{\alpha, \beta\} then
  7
                  [Case 3.1]
  8
                  \Phi_i \leftarrow \Phi_i + \lambda_{\Delta} \text{ for } i \in [i_{\min}:k]
  9
                  \Psi_j \leftarrow \Psi_j - \lambda_{\Delta} \text{ for } j \in [j_{\min} : j^*]
10
                  L_{i_{\Delta}} \leftarrow -1, L_k \leftarrow j^*
11
                  for i \in [i_{\Delta} + 1 : k - 1] do
12
                   L_i \leftarrow L_i - 1
13
                 return
14
            else if \alpha \leq \min\{\lambda_{\Delta}, \beta\} then
15
                  [Case 3.2]
16
                  \Phi_i \leftarrow \Phi_i + \alpha \text{ for } i \in [i_{\min} : k]
17
                  \Psi_j \leftarrow \Psi_j - \alpha \text{ for } j \in [j_{\min}:j^*]
18
                  L_k \leftarrow j^* + 1
19
                 return
20
            else
\mathbf{21}
                  \Phi_i \leftarrow \Phi_i + \beta \text{ for } i \in [i_{\min} : k]
22
                  \Psi_j \leftarrow \Psi_j - \beta \text{ for } j \in [j_{\min} : j^*]
23
                  if j_{min} - 1 unassigned then
24
                        [Case 3.3a]
25
                        L_{i_{\min}} \leftarrow j_{\min} - 1, L_k \leftarrow j^*
26
                        for i \in [i_{\min} + 1 : k - 1] do
27
                          L_i \leftarrow L_i - 1
28
                        return
29
                  else
30
                        [Case 3.3b]
31
                       i_{\min} \leftarrow i_{\min} - 1, j_{\min} \leftarrow j_{\min} - 1
32
```

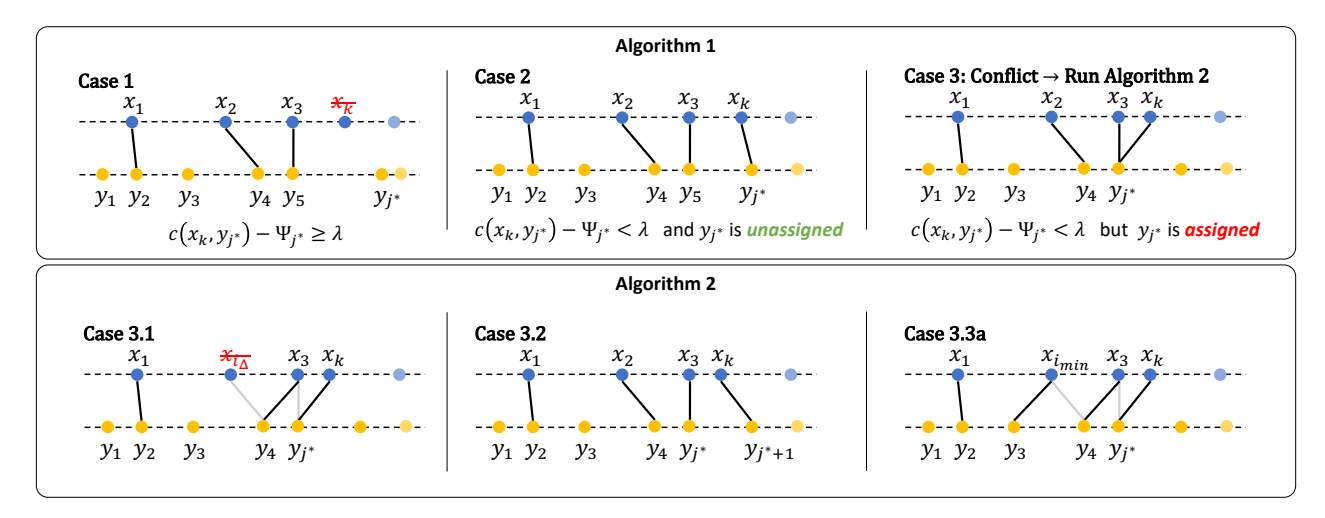


Figure 1: Depiction of Algorithms 1 and 2 for solving the optimal partial transport in one dimension.

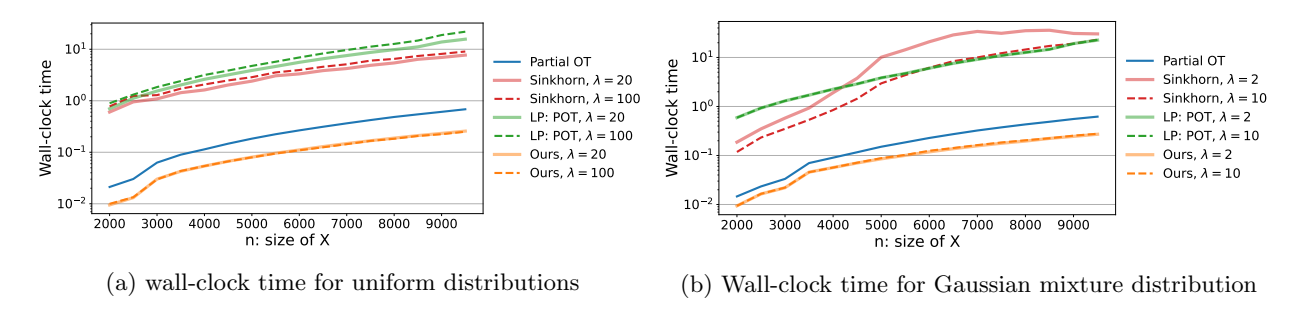


Figure 2: We test the wall-clock time of our Algorithm 1, the partial OT solver (Algorithm 1 in [4]), the unbalanced Sinkhorn algorithm [11], and the linear programming solver in POT [22], which is written in C. The maximum number of iterations for linear programming is set to 100n and it has been reached several times in the experiment.

 $\frac{1}{5}\sum_{k=1}^{5}\mathcal{N}(-4+2k,1),\{y_j\}_{j=1}^{m}\stackrel{\text{iid}}{\sim}\frac{1}{6}\sum_{k=1}^{6}\mathcal{N}(-5+2k,1),\ \lambda\in\{2,10\},\ n\in\{2000,2500,\dots10000\},\ \text{and}\ m=n+1000.$ We compare our algorithm with POT (Algorithm 1 in [4]), an unbalanced Sinkhorn algorithm [11] (we set the entropic regularization parameter to $\lambda/40$), and linear programming in python OT [22]. Our algorithm, POT and Sinkhorn algorithm are accelerated by numba and linear programming is written in C++. Note that POT [4] and the unbalanced Sinkhorn minimize a different model. In addition, for the latter the performance depends strongly on the strength of regularization and we found that it was not competitive in the regime of low blur. For each (n,m), we repeat the computation 10 times and compute the average. For our method and POT, the time of sorting is included, and for the linear programming and Sinkhorn algorithms, the time of computing the cost matrix is included. We also visualize our algorithm's solutions for $\{x_i\}_{i=1}^n \stackrel{\text{iid}}{\sim} \text{Unif}(-20,20),\{y_j\}_{j=1}^m \stackrel{\text{iid}}{\sim} \text{Unif}(-40,40), n=8, m=16 \text{ and } \lambda\in\{1,10,100,1000\}$ (see figure 3). One can observe that as λ increases larger transportations are permitted. The data type is 32-bit float number and the experiments are conducted on a Linux computer with AMD EPYC 7702P CPU with 64 cores and 256GB DDR4 RAM.

5 Sliced Optimal Partial Transport

In practice, data has multiple dimensions and the 1-D computational methods cannot be applied directly. In the balanced OT setting the sliced OT approach [45, 5, 31, 33, 30] applies the 1-D OT solver on projections (i.e., slices) of two r-dimensional distributions. Inspired by these works, we extend the sliced OT technique into the OPT setting and introduce the so-called "sliced-unbalanced optimal transport" problem.

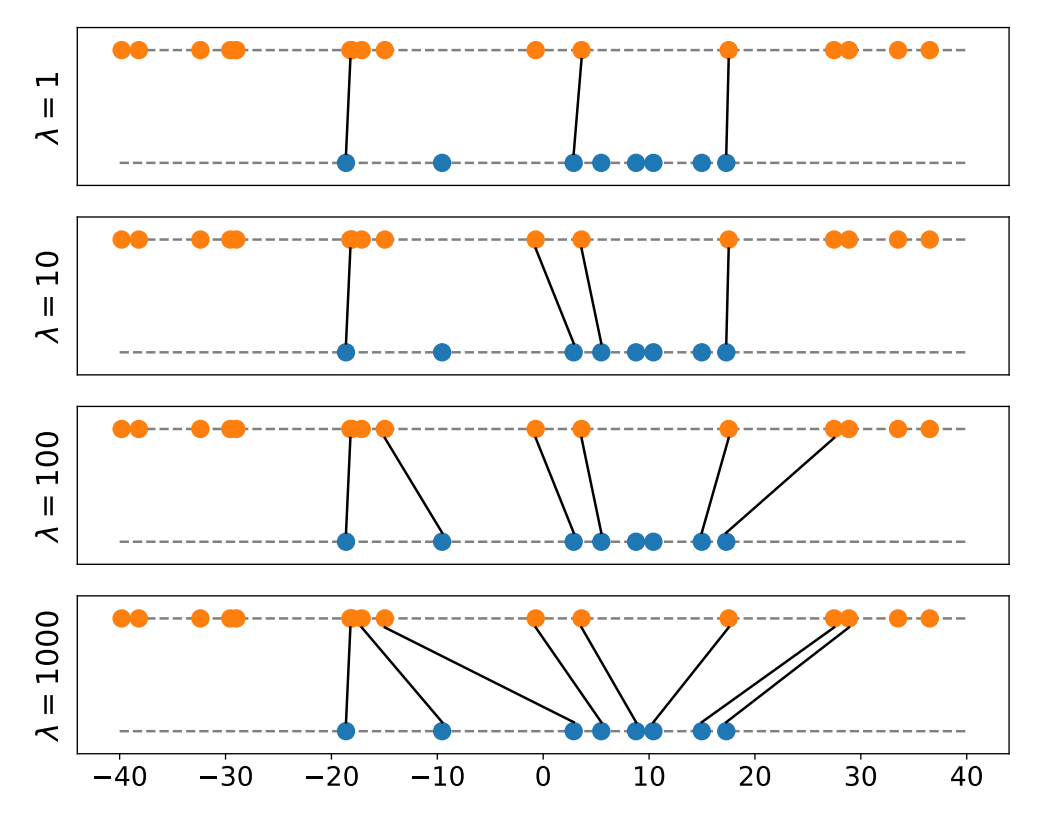


Figure 3: Output of the proposed algorithm for $\lambda \in [1, 10, 100, 1000]$ on a sample pair of measures.

Definition 5.1. In \mathbb{R}^r space, given $\mu, \nu \in \mathcal{M}_+(\Omega)$ where $\Omega \subset \mathbb{R}^r$ and $\lambda : \mathbb{S}^{r-1} \to \mathbb{R}_{++}$ is an L^1 function, we define the sliced optimal partial transport (SOPT) problem as follows:

$$SOPT_{\lambda}(\mu, \nu) = \int_{\mathbb{S}^{r-1}} OPT_{\lambda(\theta)}(\langle \theta, \cdot \rangle_{\#} \mu, \langle \theta, \cdot \rangle_{\#} \nu) \, d\sigma(\theta)$$
 (7)

where $\mathrm{OPT}_{\lambda}(\cdot,\cdot)$ is defined in (3), $\sigma \in \mathcal{P}(\mathbb{S}^{r-1})$ is a probability measure such that $\mathrm{supp}(\sigma) = \mathbb{S}^{r-1}$.

Generally σ is set to be the uniform distribution on the unit ball \mathbb{S}^{r-1} . Whenever $\operatorname{supp}(\sigma) = \mathbb{S}^{r-1}$, $\operatorname{SOPT}_{\lambda}(\mu, \nu)$ defines a metric.

Theorem 5.2. Suppose $c: \Omega \times \Omega \to \mathbb{R}_+$ is a metric on Ω and $\lambda \in L^1(\mathbb{S}^{r-1}; \mathbb{R}_{++})$ satisfies $\inf_{\theta \in \mathbb{S}^{r-1}} \lambda(\theta) > 0$, then $SOPT_{\lambda}(\mu, \nu)$ is a metric in $\mathcal{M}_+(\Omega)$.

In practice, this integration is usually approximated using a Monte Carlo scheme that draws a finite number of i.i.d. samples $\{\theta_l\}_{l=1}^N$ from Unif(\mathbb{S}^{d-1}) and replaces the integral with an empirical average:

$$SOPT_{\lambda}(\mu, \nu) \approx \frac{1}{N} \sum_{l=1}^{N} OPT_{\lambda_{l}}(\langle \theta_{l}, \cdot \rangle_{\#} \mu, \langle \theta_{l}, \cdot \rangle_{\#} \nu).$$

Proof of Theorem 5.2. First we claim $SOPT_{\lambda}(\cdot, \cdot) : (\mathcal{M}_{+}(\Omega))^{2} \to \mathbb{R}_{+}$ is a well defined function. It is clear $SOPT_{\lambda}(\cdot, \cdot)$ is a function with domain $\mathcal{M}_{+}(\Omega)^{2}$ and co-domain $\mathbb{R} \cup \{\pm \infty\}$. Pick μ, ν , we will show $SOPT_{\lambda} \in [0, \infty)$. We have

$$SOPT_{\lambda}(\mu, \nu) = \int_{\mathbb{S}^{d-1}} OPT_{\lambda(\theta)}(\langle \theta, \cdot \rangle_{\#} \mu, (\langle \theta, \cdot \rangle_{\#} \nu) \, d\sigma(\theta) \ge 0$$
(8)

where the inequality follows from the fact $\mathrm{OPT}\lambda(\theta)(\langle \theta, \cdot \rangle_{\#}\mu, (\langle \theta, \cdot \rangle_{\#}\nu) \geq 0, \forall \theta$. It remains to show $\mathrm{SOPT}_{\lambda}(\mu, \nu) < \infty$. We have

$$\begin{aligned} \mathrm{SOPT}_{\lambda}(\mu,\nu) &\leq \int_{\mathbb{S}^{d-1}} \frac{1}{2} \lambda(\theta) (\|\langle \theta, \cdot \rangle_{\#} \mu\|_{\mathrm{TV}} + \|\langle \theta, \cdot \rangle_{\#} \nu\|_{\mathrm{TV}}) \, \mathrm{d}\sigma(\theta) \\ &= \frac{1}{2} (\mu(\Omega) + \nu(\Omega)) \int_{\mathbb{S}^{d-1}} \lambda(\theta) \, \mathrm{d}\sigma(\theta) \\ &< \infty \end{aligned}$$

where the first inequality follows by plugging zero measure into the cost function in (3); the second inequality holds since λ is an L¹ function.

Next, we will show $\mu = \nu$ iff $SOPT_{\lambda}(\mu, \nu) = 0$. If $\mu = \nu$, we have for every θ , $\langle \theta, \rangle_{\#}\mu = \langle \theta, \rangle_{\#}\nu$ and thus $OPT_{\lambda(\theta)}(\langle \theta, \cdot \rangle_{\#}\mu, \langle \theta, \cdot \rangle_{\#}\nu) = 0$. Therefore $SOPT_{\lambda}(\mu, \nu) = 0$. For the reverse direction, we suppose $SOPT_{\lambda}(\mu, \nu) = 0$. Since $SOPT_{\lambda}(\mu, \nu) = 0$. Since $SOPT_{\lambda(\theta)}(\langle \theta, \cdot \rangle_{\#}\mu, \langle \theta, \cdot \rangle_{\#}\nu) = 0$. For almost every θ , since $SOPT_{\lambda(\theta)}(\nu, \cdot)$ is a metric (see [12, Proposition 2.10] or [43, Proposition 5]), we have $SOPT_{\lambda(\theta)}(\nu, \cdot)$ By the injectivity of Radon transform on measures (see [5, Proposition 7]), we have $SOPT_{\lambda(\theta)}(\nu, \cdot)$ By the injectivity of Radon transform on measures (see [5, Proposition 7]),

For symmetry, we have

$$SOPT_{\lambda}(\mu, \nu) = \int_{\mathbb{S}^{d-1}} OPT_{\lambda(\theta)}(\langle \theta, \cdot \rangle_{\#} \mu, \langle \theta, \rangle_{\#} \nu) d\sigma(\theta)$$

$$= \int_{\mathbb{S}^{d-1}} OPT_{\lambda(\theta)}(\langle \theta, \cdot \rangle_{\#} \nu, \langle \theta, \cdot \rangle_{\#} \mu) d\sigma(\theta)$$

$$= SOPT_{\lambda}(\nu, \mu)$$
(9)

where the second equality follows from the fact $\mathrm{OPT}_{\lambda(\theta)}(\cdot,\cdot)$ is a metric for each θ . For the triangle inequality, we choose μ_1, μ_2, μ_3 and have:

$$SOPT_{\lambda}(\mu_{1}, \mu_{3}) = \int_{\mathbb{S}^{d-1}} OPT_{\lambda(\theta)}(\langle \theta, \cdot \rangle_{\#} \mu_{1}, \langle \theta, \cdot \rangle_{\#} \mu_{3}) \, d\sigma(\theta)$$

$$\leq \int_{\mathbb{S}^{d-1}} \left[OPT_{\lambda(\theta)}(\langle \theta, \cdot \rangle_{\#} \mu_{1}, \langle \theta, \cdot \rangle_{\#} \mu_{2}) + OPT_{\lambda(\theta)}(\langle \theta, \cdot \rangle_{\#} \mu_{2}, \langle \theta, \cdot \rangle_{\#} \mu_{3}) \right] \, d\sigma(\theta)$$

$$= \left(\int_{\mathbb{S}^{d-1}} OPT_{\lambda(\theta)}(\langle \theta, \cdot \rangle_{\#} \mu_{1}, \langle \theta, \cdot \rangle_{\#} \mu_{2}) \, d\sigma(\theta) \right) + \left(\int_{\mathbb{S}^{d-1}} OPT_{\lambda(\theta)}(\langle \theta, \cdot \rangle_{\#} \mu_{1}, \langle \theta, \cdot \rangle_{\#} \mu_{2}) \, d\sigma(\theta) \right)$$

$$= SOPT_{\lambda}(\mu_{1}, \mu_{2}) + SOPT_{\lambda}(\mu_{2}, \mu_{3})$$

where the first inequality follows from the fact $OPT_{\lambda(\theta)}(\cdot, \cdot)$ is a metric for each θ .

6 Applications

6.1 Point Cloud Registration

Point cloud registration is a transformation estimation problem between two point clouds, which is a critical problem in numerous computer vision applications [51, 27]. In particular, given two 3-D point clouds, $x_i \sim \mu$, $i=1,\ldots,n$ and $y_j \sim \nu$, $j=1,\ldots,m$, one assumes there is an unknown mapping, T, that satisfies $\nu=T_{\#}\mu$. In many applications, the mapping T is restricted to have the following form, $Tx=sRx+\beta$, where R is a 3×3 dimensional rotation matrix, s>0 is the scaling and β , called translation vector, is 3×1 vector. The goal is then to estimate the transform, T, based on the two point clouds.

The classic approach for solving this problem is Iterative Closest Point Algorithms (ICP) introduced by [9, 3]. By [53]'s work, classical ICP can be extended into the uniformly scaled setting, with further developments by [17]. To address the some issues of ICP methods (convergence to local minimum, poor performance when the size of the two datasets are not equal), [4] proposed the Fast Iterative Sliced Transport algorithm (FIST) using sliced partial optimal transport (SPOT).

Problem setup and our method. We consider the uniform scaled point cloud registration problem and assume a subset of points in both the source and target point clouds are corrupted with additional uniformly

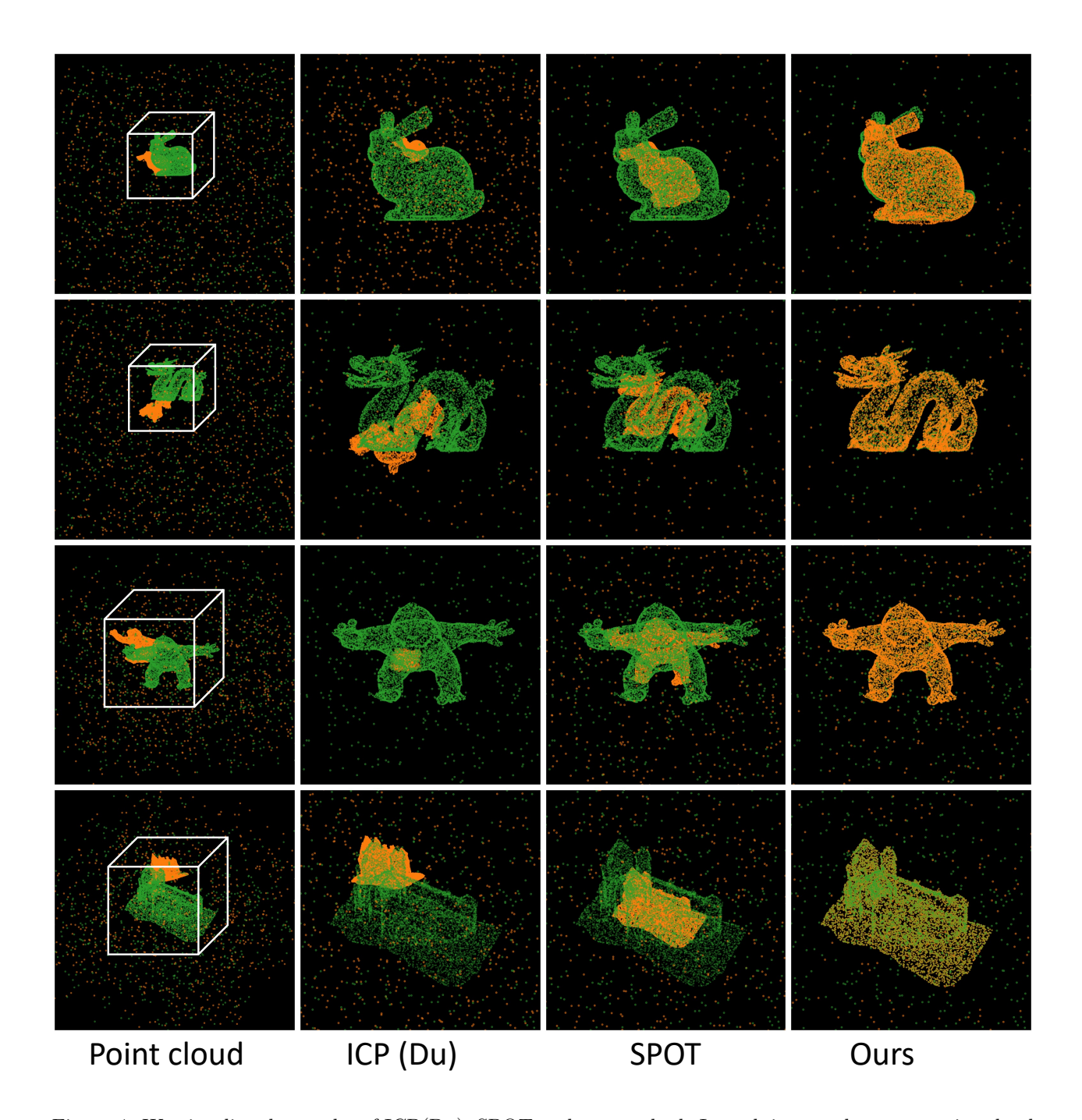


Figure 4: We visualize the results of ICP(Du), SPOT and our method. In each image, the target point cloud is in green and source point cloud is in orange.

	$10\mathrm{k,}5\%$	$10\mathrm{k,}7\%$	$9\mathrm{k,}5\%$	$9\mathrm{k}{,}7\%$
ICP-D	1.10(1.59)	3.60(0.11)		
ICP-U	3.72(0.53)	3.72(0.52)	3.69(0.63)	3.92(0.32)
SPOT	1.27(0.01)		1.42(0.13)	
Ours	0.01(1e-3)	0.02(2e-3)	0.20(0.09)	0.33(0.03)

Table 1: We compute the mean (and variance, in parenthesis) of errors in the Frobenius norm between the ground truth and estimated transportation matrices for ICP(Du), ICP(Umeyama), SPOT and our method. We vary the size of the source point cloud from 9k to 10k samples, the percentage of noise from 5% to 7% (on both source and target datasets).

			ICP		SPOT		Ours	
Dataset	Source	Target	${\bf Time/iter.}$	# Iter.	Time/iter.	# Iter.	${\bf Time/iter.}$	# Iter.
Bunny (5%) Bunny (7%)	$9k \\ 10k$	$10k \\ 10k$	$\begin{array}{ c c }\hline 0.66s\\ 0.76s\end{array}$	50 130	$\begin{array}{ c c c }\hline 10.9s\\ 13.2s\end{array}$	100 100	$\begin{array}{ c c }\hline 0.31s\\ 0.35s\end{array}$	2000 2000
Dragon (5%) Dragon (7%)	$9k \\ 10k$	$10k \\ 10k$	$\begin{array}{ c c }\hline 0.66s\\ 0.77s\end{array}$	100 100	$\begin{vmatrix} 10.4s \\ 13.1s \end{vmatrix}$	100 80	$\begin{array}{ c c c }\hline 0.31s\\ 0.35s\end{array}$	2000 1500
Mumble (5%) Mumble (7%)	$9k \\ 10k$	$10k \\ 10k$	$\begin{array}{ c c }\hline 0.65s\\ 0.78s\end{array}$	100 100	$\begin{vmatrix} 10.78s \\ 13.18s \end{vmatrix}$	100 80	$\begin{vmatrix} 0.32s \\ 0.36s \end{vmatrix}$	2000 1500
Castle (5%) Castle (7%)	$9k \\ 10k$	$10k \\ 10k$	0.66s $0.76s$	150 350	$\begin{array}{ c c c }\hline 10.7s\\ 13.7s\end{array}$	100 80	$\begin{array}{ c c }\hline 0.31s\\ 0.35s\end{array}$	2000 1800

Table 2: This table reports the data for our method in shape registration experiment: the number of source and target distribution, the percentage of noise, the computation times per iteration and numbers of iterations they took to converge for ICP(Du), SPOT, and our method. The source point cloud is in orange color and the target is in blue. The percentage of noise is given in brackets next to the dataset name.

distributed noise. We suppose prior knowledge of the proportion of noise is given (i.e., we have prior knowledge of the number of clean data).

In general, the registration problem can be iteratively solved and each iteration contains two steps: estimating the correspondence and computing the optimal transform from corresponding points. The second step has a closed-form solution. For the first step, the ICP method estimates the correspondence by finding the closest y for each transformed x. Inspired by this work, we estimate the correspondence by using our SOPT solver. See Algorithm 3.

```
Algorithm 3: iterative-sopt
```

```
Input: \{x_i\}_{i=1}^n, \{y_j\}_{j=1}^m, n_0:the # of clean x, N: # of projections
1 initialize R, s, \beta, \lambda, sample \{\theta_i\}_{i=1}^N \subset \mathbb{S}^2
2 for l = 1, ... N do
        \hat{Y} \leftarrow sRX + \beta
3
        Compute transportation plan L of OPT_{\lambda}(\theta_l^T \hat{Y}, \theta_l^T Y) by algorithm 1
4
        \forall i \in \text{dom}(L), \ \hat{y}_i \leftarrow \hat{y}_i + (\theta_l^T y_{L[i]} - \theta_l^T \hat{y}_i)\theta
5
        Compute R, s, \beta from (X[dom(L)], \hat{Y}[dom(L)]) by ICP (e.g., equations (39)-(42) in [53])
        If |dom(L)| > n_0, decrease \lambda; otherwise, increase \lambda.
```

Experiment. We illustrate our algorithm on different 3D point clouds, including Stanford Bunny, Stanford dragon, Witch-castle and Mumble Sitting. For each dataset, we generate transforms by uniformly sampling angles from $[-1/3\pi, 1/3\pi]$, translations from [-2std, 2std], and scalings from [0, 2], where std is the standard deviation of the dataset. Then we sample noise uniformly from the region $[-M, M]^3$ where

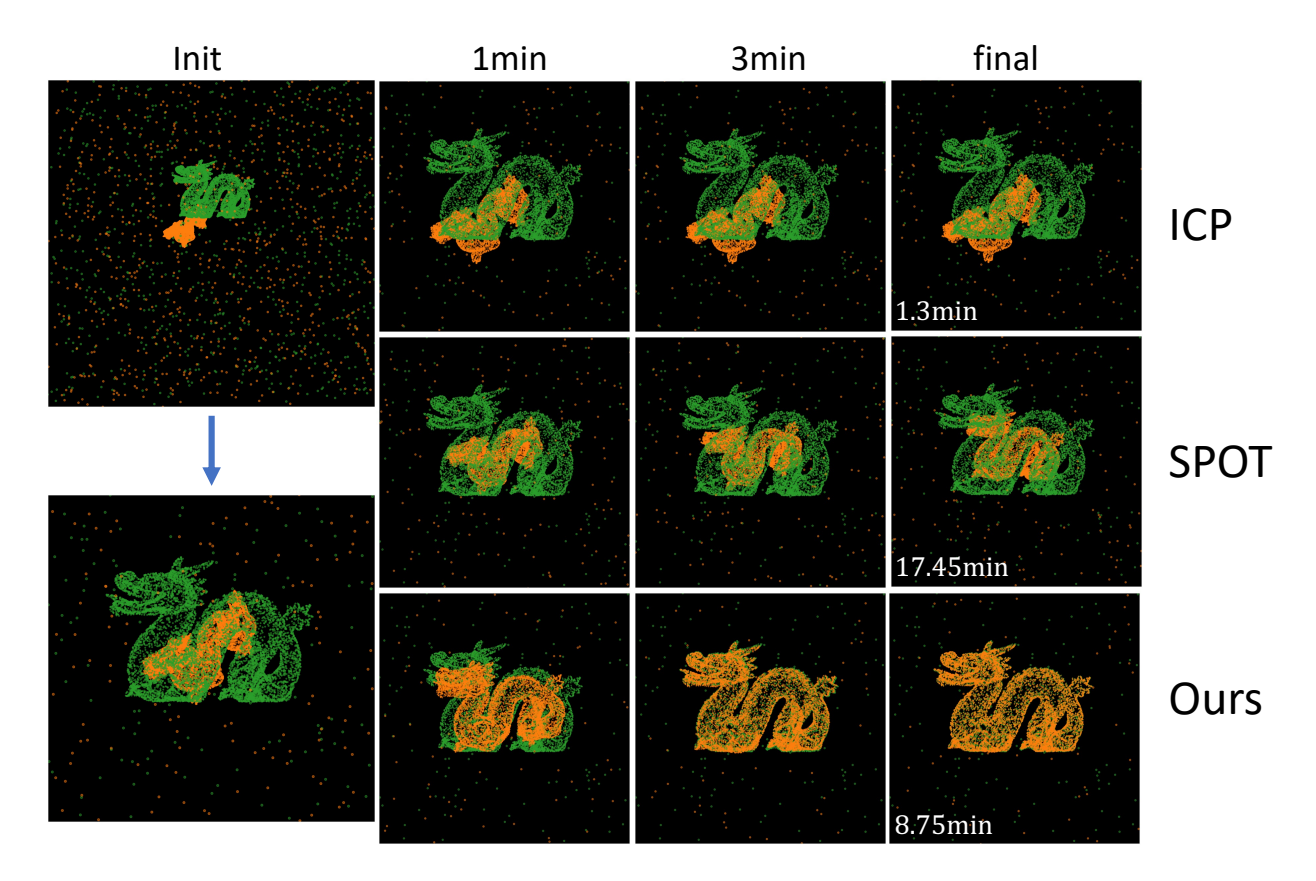


Figure 5: We visualize the processed point cloud for every method with respect to time. The dataset is Stanford dragon. In each image, the point cloud in orange is the source and the point cloud in green color is the target.

 $M = \max_{i \in [1:n]}(||x_i||)$ and concatenate it to our point clouds. The number of points in the target (clean) data is fixed to be 10k and we vary the number of points in the source (clean) data from 9k to 10k, and the percentage of noise from 5% to 7%.

Performance. For accuracy, we compute the average and standard deviation of error defined by the Frobenius norm between the estimated transformation and the ground truth (see Table 1). For accuracy, we observe ICP methods systematically fail, since the nearest neighbor matching technique induces a non-injective correspondence, which may result in a too-small scaling factor. SPOT can successfully recover the rotation, but it fails to recover the scaling. Our method is the only one that recovers the ground truth for the noise-corrupted data (since it utilizes prior knowledge).

For running time, ICP has the fastest convergence time which is generally 100-260 seconds since finding the correspondence by the closest neighbor can be done immediately after the cost matrix is computed. SPOT requires 1000-1300 seconds and our method requires 500-700 seconds. The data type is 32-bit float number and the experiment is conducted on a Linux computer with AMD EPYC 7702P CPU with 64 cores and 256GB DDR4 RAM.

6.2 Color Adaptation

Transferring colors between images is a classical task in computer vision and image science. Given two images, the goal is to impose on one of the images (source image) the histogram of the other image (target image). Optimal transport-based approaches have been developed and achieved great success in this task [11, 5, 45, 19]. However, in the balanced OT setting, the OT-based approach requires normalizing the histograms of (sampled) colors, which may lead to undesired performance. For example, suppose the majority of a target image is red, (e.g. an image of evening sunset) and the majority of a source image is green (e.g. image of trees).

Then balanced-OT-based approaches will produce a red tree in the result. To address this issue, [4] applied the SPOT-based approach which will match all the pixels in the source image to *partial* pixels in the target image.

Our method. Inspired by [19, 4], our method contains the following three steps: First, we sample pixels from the source and target image by k-mean clustering (or another sampling method). Second, we transport the sampled source pixels into the target domain. If OT or entropic OT is applied, it can be done by the optimal transportation plan; if sliced-OT is applied, the source pixels would be updated iteratively for each slice based on the gradient of 1-D OT with respect to the source pixels (see equation (46) in [5], or line 5 in our algorithm 3). In our method, we apply the transportation plan from OPT. Third, we reconstruct the source image based on the transported source pixels (e.g. see Equation 4.1 in [19]).

Experiment. We first normalize all the pixels in the source and target images to be in the range [0, 1], then we use k-means clustering to sample 5000 pixels from the source image and 10000 pixels from the target image. We compare the performance of the OT-based and Entropic-OT-based domain adaptation functions in PythonOT [22] (ot.da.EMDTransport and ot.da.SinkhornTransport) whose solver of OT is written in C++
*, SPOT [4] and our method based on sliced optimal partial transport. For our method, we test it in two schemes, $\lambda = 10.0$ and $\lambda < 2.0$. In the first case, λ achieves the maximum distance of two (normalized) pixels, that is, we will transport all the source pixels into the target domain. In the second case, we choose small λ , and theoretically, only partial source pixels will be transported into the target domain.

Performance. In these examples, the OT-based approach which matches all (sampled) pixels of the source image to all pixels of a target image can lead to undesired results. For example, in the second row of Figure 6, the third image has dark blue in the sky and red color on the ground. This issue is alleviated in SPOT and our method. In our method, when $\lambda = 5.0$, we will transfer all the (sampled) pixels from source to target and the result is similar to the result of SPOT *. When $\lambda < 2.0$, the resulting image is closer to the source image. The OT-based method requires 40-50 seconds (we set the maximum iteration number of linear programming to be 1000,000); the Partial OT method requires 80-90 seconds (the # of projections is set to be 400) and our method requires 60-80 seconds (the # of projections is set to be 400). The data type is 32-bit float number and the experiment is conducted on a Linux computer with AMD EPYC 7702P CPU with 64 cores and 256GB DDR4 RAM.

7 Conclusion and future work

This paper proposes a fast computational method for solving the OPT problem for one-dimensional discrete measures. We provide computational and wall-clock analysis experiments to assess our proposed algorithm's correctness and computational benefits. Then, utilizing one-dimensional slices of an r-dimensional measure we propose the "sliced optimal partial transport (SOPT)" distance. Beyond our theoretical and algorithmic contributions, we provide empirical evidence that SOPT is practical for large-scale applications like point cloud registration and image color adaptation. In point cloud registration, we show that compared with other classical methods, our SOPT-based approach adds robustness when the source and target point clouds are corrupted by noise. In the future, we will investigate the potential applications of SOPT in other machine learning tasks such as open set domain adaptation problems and measuring task similarities in continual and curriculum learning.

8 Acknowledgment

The authors thank Rana Muhammad Shahroz Khan for helping in code testing and thank Dr. Hengrong Du (hengrong.du@vanderbilt.edu) for helpful discussions. This work was partially supported by the Defense Advanced Research Projects Agency (DARPA) under Contract No. HR00112190132. MT was supported by the European Research Council under the European Union's Horizon 2020 research and innovation programme Grant Agreement No. 777826 (NoMADS).

^{*}We modify their code to increase the speed.

^{*}We conjecture the two results are not exactly the same due to the randomness of projections.

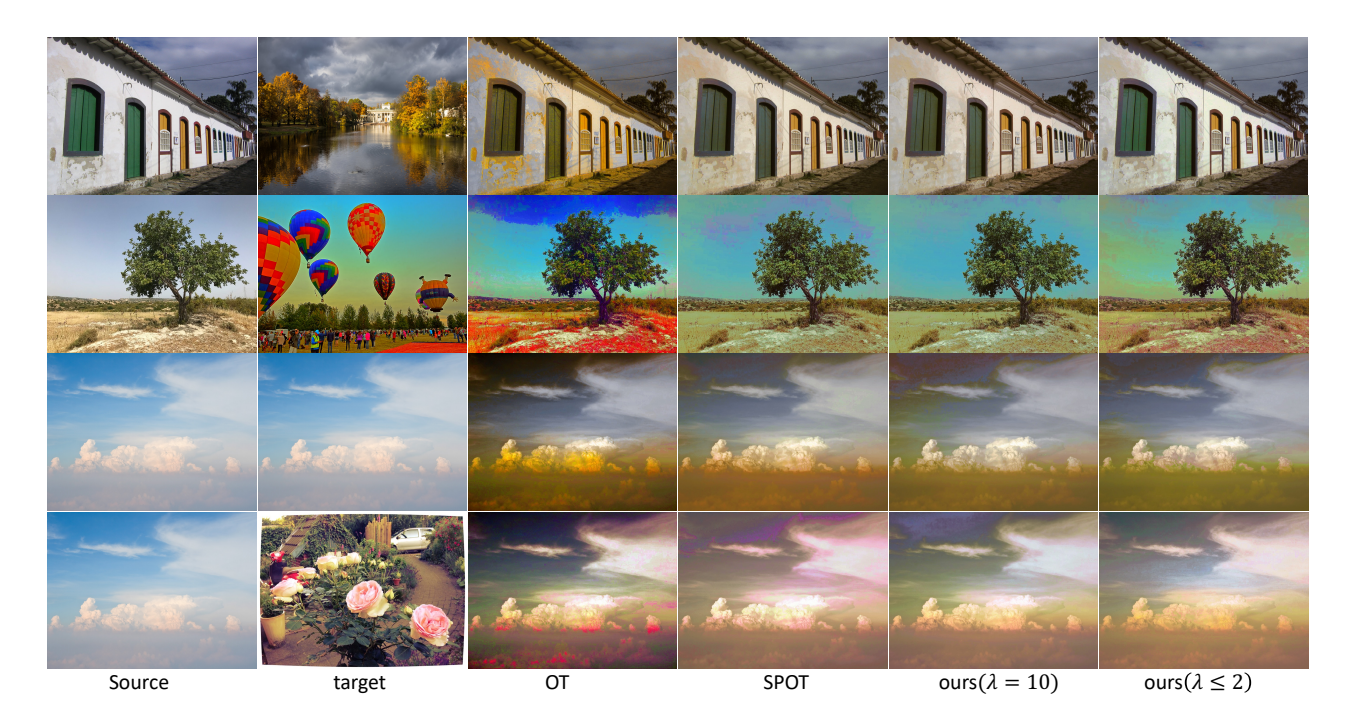


Figure 6: We transfer colors from source image to the target image by the methods based on optimal transport [19], SPOT [4] and our SOPT. For our method, we set $\lambda = 10$ and a small value less than 2. Image via Flickr: Facade by Phil Whitehouse, palace by Neil Williamson, clouds by Tim Wang, air balloon by Kirt Edblom, roses by Felix Schaumburg.

References

- [1] Martin Arjovsky, Soumith Chintala, and Léon Bottou. Wasserstein generative adversarial networks. In *International conference on machine learning*, pages 214–223. PMLR, 2017. 1
- [2] Jean-David Benamou, Guillaume Carlier, Marco Cuturi, Luca Nenna, and Gabriel Peyré. Iterative bregman projections for regularized transportation problems. SIAM Journal on Scientific Computing, 37(2):A1111-A1138, 2015.
- [3] Paul J Besl and Neil D McKay. Method for registration of 3-d shapes. In Sensor fusion IV: control paradigms and data structures, volume 1611, pages 586–606. Spie, 1992. 11
- [4] Nicolas Bonneel and David Coeurjolly. SPOT: sliced partial optimal transport. ACM Transactions on Graphics, 38(4):1–13, 2019. 2, 7, 9, 11, 15, 16
- [5] Nicolas Bonneel, Julien Rabin, Gabriel Peyré, and Hanspeter Pfister. Sliced and Radon Wasserstein barycenters of measures. *Journal of Mathematical Imaging and Vision*, 51(1):22–45, 2015. 2, 9, 11, 14, 15
- [6] R. E. Burkhard, B. Klinz, and R. Rudolf. Perspectives of Monge properties in optimization. Discr. Appl. Math., 70(2):95-161, 1996. 20
- [7] Luis A Caffarelli and Robert J McCann. Free boundaries in optimal transport and monge-ampere obstacle problems. *Annals of mathematics*, pages 673–730, 2010. 1, 2, 19
- [8] Yongxin Chen, Tryphon T Georgiou, Lipeng Ning, and Allen Tannenbaum. Matricial wasserstein-1 distance. *IEEE control systems letters*, 1(1):14–19, 2017. 3
- [9] Yang Chen and Gérard Medioni. Object modelling by registration of multiple range images. *Image and vision computing*, 10(3):145–155, 1992. 11
- [10] Lenaic Chizat, Gabriel Peyré, Bernhard Schmitzer, and François-Xavier Vialard. An interpolating distance between optimal transport and Fisher-Rao metrics. Foundations of Computational Mathematics, 18(1):1-44, 2018. 1, 19
- [11] Lenaic Chizat, Gabriel Peyré, Bernhard Schmitzer, and François-Xavier Vialard. Scaling algorithms for unbalanced optimal transport problems. *Mathematics of Computation*, 87(314):2563–2609, 2018. 1, 2, 9, 14
- [12] Lenaic Chizat, Gabriel Peyré, Bernhard Schmitzer, and François-Xavier Vialard. Unbalanced optimal transport: Dynamic and Kantorovich formulations. *Journal of Functional Analysis*, 274(11):3090-3123, 2018. 1, 3, 11, 19

- [13] Nicolas Courty, Rémi Flamary, Amaury Habrard, and Alain Rakotomamonjy. Joint distribution optimal transportation for domain adaptation. Advances in Neural Information Processing Systems, 30, 2017. 1
- [14] Nicolas Courty, Rémi Flamary, and Devis Tuia. Domain adaptation with regularized optimal transport. In Joint European Conference on Machine Learning and Knowledge Discovery in Databases, pages 274–289. Springer, 2014. 1
- [15] Marco Cuturi. Sinkhorn distances: Lightspeed computation of optimal transport. Advances in neural information processing systems, 26, 2013. 1, 2
- [16] Ishan Deshpande, Yuan-Ting Hu, Ruoyu Sun, Ayis Pyrros, Nasir Siddiqui, Sanmi Koyejo, Zhizhen Zhao, David Forsyth, and Alexander G Schwing. Max-sliced wasserstein distance and its use for gans. In Proceedings of the IEEE/CVF Conference on Computer Vision and Pattern Recognition, pages 10648–10656, 2019.
- [17] Shaoyi Du, Nanning Zheng, Shihui Ying, Qubo You, and Yang Wu. An extension of the icp algorithm considering scale factor. In 2007 IEEE International Conference on Image Processing, volume 5, pages V-193. IEEE, 2007.
- [18] Kilian Fatras, Thibault Séjourné, Rémi Flamary, and Nicolas Courty. Unbalanced minibatch optimal transport; applications to domain adaptation. In *International Conference on Machine Learning*, pages 3186–3197. PMLR, 2021. 1
- [19] Sira Ferradans, Nicolas Papadakis, Gabriel Peyré, and Jean-François Aujol. Regularized discrete optimal transport. SIAM Journal on Imaging Sciences, 7(3):1853–1882, 2014. 14, 15, 16
- [20] Alessio Figalli. The optimal partial transport problem. Archive for rational mechanics and analysis, 195(2):533–560, 2010. 1, 3, 4, 19
- [21] Alessio Figalli and Nicola Gigli. A new transportation distance between non-negative measures, with applications to gradients flows with dirichlet boundary conditions. *Journal de mathématiques pures et appliquées*, 94(2):107–130, 2010. 1, 3, 19
- [22] Rémi Flamary, Nicolas Courty, Alexandre Gramfort, Mokhtar Z. Alaya, Aurélie Boisbunon, Stanislas Chambon, Laetitia Chapel, Adrien Corenflos, Kilian Fatras, Nemo Fournier, Léo Gautheron, Nathalie T.H. Gayraud, Hicham Janati, Alain Rakotomamonjy, Ievgen Redko, Antoine Rolet, Antony Schutz, Vivien Seguy, Danica J. Sutherland, Romain Tavenard, Alexander Tong, and Titouan Vayer. Pot: Python optimal transport. Journal of Machine Learning Research, 22(78):1–8, 2021. 9, 15
- [23] Charlie Frogner, Chiyuan Zhang, Hossein Mobahi, Mauricio Araya, and Tomaso A Poggio. Learning with a Wasserstein loss. Advances in neural information processing systems, 28, 2015. 1
- [24] Aude Genevay, Marco Cuturi, Gabriel Peyré, and Francis Bach. Stochastic optimization for large-scale optimal transport. Advances in neural information processing systems, 29, 2016. 2
- [25] Aude Genevay, Gabriel Peyré, and Marco Cuturi. GAN and VAE from an optimal transport point of view. arXiv preprint arXiv:1706.01807, 2017. 1
- [26] Kevin Guittet. Extended Kantorovich norms: a tool for optimization. PhD thesis, INRIA, 2002. 1, 2
- [27] Xiaoshui Huang, Guofeng Mei, Jian Zhang, and Rana Abbas. A comprehensive survey on point cloud registration. arXiv preprint arXiv:2103.02690, 2021. 11
- [28] Leonid V Kantorovich. On a problem of monge. In CR (Doklady) Acad. Sci. URSS (NS), volume 3, pages 225–226, 1948. 2, 3
- [29] Narendra Karmarkar. A new polynomial-time algorithm for linear programming. In *Proceedings of the sixteenth annual ACM symposium on Theory of computing*, pages 302–311, 1984. 2
- [30] Soheil Kolouri, Kimia Nadjahi, Umut Simsekli, Roland Badeau, and Gustavo Rohde. Generalized sliced Wasserstein distances. Advances in Neural Information Processing Systems, 32, 2019. 2, 9
- [31] Soheil Kolouri, Se Rim Park, and Gustavo K Rohde. The radon cumulative distribution transform and its application to image classification. *IEEE transactions on image processing*, 25(2):920–934, 2015. 2, 9
- [32] Soheil Kolouri, Se Rim Park, Matthew Thorpe, Dejan Slepcev, and Gustavo K Rohde. Optimal mass transport: Signal processing and machine-learning applications. *IEEE signal processing magazine*, 34(4):43–59, 2017. 1
- [33] Soheil Kolouri, Yang Zou, and Gustavo K Rohde. Sliced wasserstein kernels for probability distributions. In Proceedings of the IEEE Conference on Computer Vision and Pattern Recognition, pages 5258–5267, 2016. 2, 9
- [34] Tam Le, Makoto Yamada, Kenji Fukumizu, and Marco Cuturi. Tree-sliced variants of wasserstein distances. Advances in neural information processing systems, 32, 2019.
- [35] Wonjun Lee, Rongjie Lai, Wuchen Li, and Stanley Osher. Generalized unnormalized optimal transport and its fast algorithms. *Journal of Computational Physics*, 436:110041, 2021. 3, 19
- [36] Jan Lellmann, Dirk A Lorenz, Carola Schonlieb, and Tuomo Valkonen. Imaging with kantorovich–rubinstein discrepancy. SIAM Journal on Imaging Sciences, 7(4):2833–2859, 2014. 1
- [37] Matthias Liero, Alexander Mielke, and Giuseppe Savare. Optimal entropy-transport problems and a new Hellinger-Kantorovich distance between positive measures. *Inventiones mathematicae*, 211(3):969–1117, 2018. 1, 3, 5, 6, 19

- [38] Huidong Liu, Xianfeng Gu, and Dimitris Samaras. Wasserstein GAN with quadratic transport cost. In Proceedings of the IEEE/CVF international conference on computer vision, pages 4832–4841, 2019.
- [39] Antoine Liutkus, Umut Simsekli, Szymon Majewski, Alain Durmus, and Fabian-Robert Stöter. Sliced-wasserstein flows: Nonparametric generative modeling via optimal transport and diffusions. In *International Conference on Machine Learning*, pages 4104–4113. PMLR, 2019.
- [40] Grégoire Montavon, Klaus-Robert Müller, and Marco Cuturi. Wasserstein training of restricted Boltzmann machines. Advances in Neural Information Processing Systems, 29, 2016. 1
- [41] James Orlin. A faster strongly polynomial minimum cost flow algorithm. In *Proceedings of the Twentieth annual ACM symposium on Theory of Computing*, pages 377–387, 1988. 2
- [42] Gabriel Peyré, Marco Cuturi, et al. Computational optimal transport: With applications to data science. Foundations and Trends® in Machine Learning, 11(5-6):355-607, 2019.
- [43] Benedetto Piccoli and Francesco Rossi. Generalized wasserstein distance and its application to transport equations with source. Archive for Rational Mechanics and Analysis, 211(1):335–358, 2014. 3, 11, 19
- [44] Benedetto Piccoli and Francesco Rossi. On properties of the generalized wasserstein distance. Archive for Rational Mechanics and Analysis, 222(3):1339–1365, 2016. 19
- [45] Julien Rabin, Gabriel Peyré, Julie Delon, and Marc Bernot. Wasserstein barycenter and its application to texture mixing. In *International Conference on Scale Space and Variational Methods in Computer Vision*, pages 435–446. Springer, 2011. 2, 9, 14
- [46] Filippo Santambrogio. Optimal Transport for Applied Mathematicians, volume 87 of Progress in Nonlinear Differential Equations and Their Applications. Birkhäuser Boston, 2015. 3
- [47] Ryoma Sato, Marco Cuturi, Makoto Yamada, and Hisashi Kashima. Fast and robust comparison of probability measures in heterogeneous spaces. arXiv preprint arXiv:2002.01615, 2020. 1, 2
- [48] Richard Sinkhorn. A relationship between arbitrary positive matrices and doubly stochastic matrices. *The annals of mathematical statistics*, 35(2):876–879, 1964. 1, 2
- [49] Justin Solomon, Fernando De Goes, Gabriel Peyré, Marco Cuturi, Adrian Butscher, Andy Nguyen, Tao Du, and Leonidas Guibas. Convolutional Wasserstein distances: Efficient optimal transportation on geometric domains. ACM Transactions on Graphics (ToG), 34(4):1–11, 2015. 1
- [50] Justin Solomon, Raif Rustamov, Leonidas Guibas, and Adrian Butscher. Wasserstein propagation for semisupervised learning. In *International Conference on Machine Learning*, pages 306–314. PMLR, 2014.
- [51] Richard Szeliski. Computer vision: algorithms and applications. Springer Science & Business Media, 2010. 11
- [52] Ilya Tolstikhin, Olivier Bousquet, Sylvain Gelly, and Bernhard Schoelkopf. Wasserstein auto-encoders. arXiv preprint arXiv:1711.01558, 2017.
- [53] Shinji Umeyama. Least-squares estimation of transformation parameters between two point patterns. *IEEE Transactions on Pattern Analysis & Machine Intelligence*, 13(04):376–380, 1991. 11, 13
- [54] Cedric Villani. Optimal transport: old and new. Springer, 2009. 3

A Relation Between Optimal Partial Transport and Unbalanced Optimal Transport

If we replace the penalty term of (3) with a constraint, i.e. we impose the condition $\gamma(\Omega^2) \geq M$, and use the fact that $|\pi_{1\#}\gamma| = |\pi_{2\#}\gamma| = \gamma(\Omega^2)$, then (3) is closely related to the Lagrangian formulation of the following "primal problem":

Primal-OPT
$$(\mu, \nu; M) = \inf_{\gamma \in \mathcal{M}_{+}(\Omega^{2})} \int c(x, y) \, d\gamma(x, y)$$
 s.t. $\gamma(\Omega^{2}) \ge M$. (10)

This, in turn, is closely related to the optimal partial transport problem proposed by [7, 21, 20] (the difference being the mass constraint of γ is imposed as an equality $\gamma(\Omega^2) = M$ rather than a lower bound $\gamma(\Omega^2) \geq M$).

Another equivalent form of the OPT problem defined in (3) is the "generalized Wasserstein distance" in [43, 44] (We refer to [10, Proposition 1.1] and [43, Proposition 4] for their equivalence.) Recently, more systematic studies of so-called "unbalanced optimal transport" or "optimal entropy transportation" problems have been conducted, for instance in [12] and [37]. OPT, (3), can be seen as a special case of these models, see for instance [12, Theorem 5.2]. It is also well known that in addition to the static Kantorovich formulations presented here, one can also give equivalent dynamic formulations in the spirit of the Benamou–Brenier formula, e.g. [12]. Finally, a related class of models with close relations to the POT problem is discussed in [35] under the name "Generalized Unnormalized Optimal Transport" (GUOT).

B Relation Between Optimal Partial Transport and Optimal Transport

Inspired by Caffarelli et al.s' technique [7], suppose $\Omega = \mathbb{R}^r$, we introduce an *isolated point* $\hat{\infty}$ into Ω by letting $\hat{\Omega} = \Omega \cup \{\hat{\infty}\}$. Suppose $\hat{\mu} = \mu + \nu(\Omega)\delta_{\hat{\infty}}$, where $\delta_{\hat{x}}$ is the Dirac mass at $\hat{x} \in \hat{\Omega}$ and $\hat{\nu} = \nu + \mu(\Omega)\delta_{\hat{\infty}}$, $\hat{c}(x,y): \hat{\Omega} \times \hat{\Omega} \to \mathbb{R}_+$ is defined as

$$\hat{c}(x,y) := \begin{cases} c(x,y) - 2\lambda & \text{if } x,y \neq \hat{\infty} \\ 0 & \text{otherwise.} \end{cases}$$

We introduce the following optimal transport problem:

$$\inf_{\hat{\gamma} \in \Gamma(\hat{\mu}, \hat{\nu})} \int \hat{c}(x, y) \, \mathrm{d}\hat{\gamma}(x, y) \tag{11}$$

We claim there exist an equivalence between this OT problem and $OPT\lambda(\mu,\nu)$.

Proposition B.1. The mapping: $T: \Gamma_{<}(\mu,\nu) \to \Gamma(\hat{\mu},\hat{\nu})$ defined by

$$\gamma \mapsto \hat{\gamma} = \gamma + (\mu - (\pi_1)_{\#} \gamma) \otimes \delta_{\hat{\infty}} + \delta_{\hat{\infty}} \otimes (\nu - (\pi_2)_{\#} \gamma) + \gamma(\Omega^2) \delta_{\hat{\infty}, \hat{\infty}}, \tag{12}$$

is a bijection and γ is optimal in $\mathrm{OPT}_{\lambda}(\mu,\nu)$ if and only if $\hat{\gamma}$ is optimal in (11).

Proof. First we will show that $\hat{\gamma} = T(\gamma) \in \Gamma(\hat{\mu}, \hat{\nu})$ for $\gamma \in \Gamma_{\leq}(\mu, \nu)$. Pick a Borel set $A \subset \hat{\Omega}$, and suppose $\hat{\infty} \in A$. By definition $\hat{\gamma}$ is a measure define on $\hat{\Omega}^2$, then we have

$$\hat{\gamma}(A \times \hat{\Omega}) = \hat{\gamma}(A \setminus \{\hat{\infty}\} \times \Omega) + \hat{\gamma}(A \setminus \{\hat{\infty}\} \times \{\hat{\infty}\}) + \hat{\gamma}(\{\hat{\infty}\} \times \Omega) + \hat{\gamma}(\{\hat{\infty}, \hat{\infty}\})$$

$$= \gamma(A \setminus \{\hat{\infty}\} \times \Omega) + (\mu - (\pi_1)_{\#}\gamma)(A \setminus \{\hat{\infty}\}) + (\nu - (\pi_2)_{\#}\gamma)(\Omega) + \gamma(\Omega^2)$$

$$= (\pi_1)_{\#}\gamma(A \setminus \{\hat{\infty}\}) + (\mu - (\pi_1)_{\#}\gamma)(A \setminus \{\hat{\infty}\}) + \nu(\Omega) - (\pi_2)_{\#}\gamma(\Omega) + \gamma(\Omega^2)$$

$$= \mu(A \setminus \{\hat{\infty}\}) + \nu(\Omega)$$

$$= \hat{\mu}(A)$$

Similarly, if $\hat{\infty} \notin A$, we have $\hat{\gamma}(A \times \hat{\Omega}) = \mu(A) = \hat{\mu}(A)$. Thus $(\pi_1)_{\#}\hat{\gamma} = \hat{\mu}$ and similarly $(\pi_2)_{\#}\hat{\gamma} = \hat{\nu}$. Therefore $\hat{\gamma} \in \Gamma(\hat{\mu}, \hat{\nu})$.

It is obvious that the mapping T is injective since if $\gamma_1 \neq \gamma_2$ where $\gamma_1, \gamma_2 \in \Gamma_{\leq}(\mu, \nu)$, then there exists one set $B \subset \Omega^2$ such that $\gamma_1(B) \neq \gamma_2(B)$. Then $\hat{\gamma}_1(B) = \gamma_1(B) \neq \gamma_2(B) = \hat{\gamma}_2(B)$. Therefore, $\hat{\gamma}_1 \neq \hat{\gamma}_2$.

Next we will show the surjectivity of T. Pick any $\hat{\gamma} \in \Gamma(\hat{\mu}, \hat{\nu})$, define γ such that for any $B \subset \Omega^2$, $\gamma(B) = \hat{\gamma}(B)$. We have $\gamma \in \Gamma_{<}(\mu, \nu)$. Indeed, pick Borel set $A \subset \Omega$, we have

$$\gamma(A \times \Omega) = \hat{\gamma}(A \times \Omega) \le \hat{\gamma}(A \times \hat{\Omega}) = \hat{\mu}(A) = \mu(A).$$

Thus $(\pi_1)_{\#}\gamma \leq \mu$, similarly we have $(\pi_2)_{\#}\gamma \leq \nu$. Let $\hat{\gamma}_1 = T(\gamma)$. We claim $\hat{\gamma} = \hat{\gamma}_1$. Note, since $\Omega^2, \Omega \times \{\hat{\infty}\}, \{\hat{\infty}\} \times \Omega, \{\hat{\infty}, \hat{\infty}\}$ is a disjoint decomposition of $\hat{\Omega}^2$ (and all of them are measurable), it is sufficient to prove $\hat{\gamma}(B) = \hat{\gamma}_1(B)$ for any Borel set B which is a subset of these four sets.

Case 1: If $B \subset \Omega^2$, we have $\hat{\gamma}_1(B) = \gamma(B) = \hat{\gamma}(B)$.

Case 2: If $B = A \times \{\hat{\infty}\}$ where $A \subset \Omega$ is Borel set, then

$$\hat{\gamma}(B) = \hat{\gamma}(A \times \hat{\Omega}) - \hat{\gamma}(A \times \Omega)$$

$$= \hat{\mu}(A) - \gamma(A \times \Omega)$$

$$= \mu(A) - (\pi_1)_{\#}\gamma(A)$$

$$= \hat{\gamma}_1(A \times \{\hat{\infty}\}) = \hat{\gamma}_1(B)$$

Similarly, if $B = {\hat{\infty}} \times A$ for some $A \subset \Omega$, we have $\hat{\gamma}(B) = \hat{\gamma}_1(B)$.

Case 3: If $B = \{(\hat{\infty}, \hat{\infty})\}$. Note, since $\hat{\gamma}_1 \in \Gamma(\tilde{\mu}, \tilde{\nu})$ as we discussed above, then $\hat{\gamma}(\hat{\Omega}^2) = \hat{\gamma}_1(\hat{\Omega}^2)$. Additionally, by Cases 1 and 2 we have $\hat{\gamma}(\Omega \times \Omega) = \hat{\gamma}_1(\Omega \times \Omega)$, $\hat{\gamma}(\Omega \times \{\hat{\infty}\}) = \hat{\gamma}_1(\Omega \times \{\hat{\infty}\})$ and $\hat{\gamma}(\{\hat{\infty}\} \times \Omega) = \hat{\gamma}_1(\{\hat{\infty}\} \times \Omega)$. Thus

$$\hat{\gamma}(B) = \hat{\gamma}(\hat{\Omega}^2) - \hat{\gamma}(\Omega^2) - \hat{\gamma}(\Omega \times \{\hat{\infty}\}) - \hat{\gamma}(\{\hat{\infty}\} \times \Omega)$$

$$= \hat{\gamma}_1(\hat{\Omega}^2) - \hat{\gamma}_1(\Omega^2) - \hat{\gamma}_1(\Omega \times \{\hat{\infty}\}) - \hat{\gamma}_1(\{\hat{\infty}\} \times \Omega)$$

$$= \hat{\gamma}_1(B)$$
(13)

Hence, $\hat{\gamma} = \hat{\gamma}_1$ and thus that the mapping is surjective.

Finally, we will show γ is optimal in $\mathrm{OPT}_{\lambda}(\mu,\nu)$ if and only if $\hat{\gamma}$ is optimal in $\mathrm{OT}(\hat{\mu},\hat{\nu})$ (defined in (11)). We let $C(\gamma)$, $\hat{C}(\hat{\gamma})$ denote the corresponding transportation cost of γ , $\hat{\gamma}$ with respect to the OPT, OT problems, i.e.

$$\hat{C}(\hat{\gamma}) = \int \hat{c}(x,y) \, d\gamma(x,y), \qquad C(\gamma) = \int c(x,y) \, d\gamma(x,y) + \lambda \left(\mu(\Omega) - \pi_{1\#}\gamma(\Omega) + \nu(\Omega) - \pi_{2\#}\gamma(\Omega)\right). \tag{14}$$

We have $C(\gamma) = C(\hat{\gamma}) + \frac{1}{2}\lambda(\mu(\Omega) + \nu(\Omega))$. Combining with the fact the mapping is bijection, we have γ is optimal iff $\hat{\gamma}$ is optimal.

C Correctness and complexity of Algorithms 1 and 2

C.1 Correctness

In this section we prove the correctness of Algorithms 1 and 2 as stated above and we discuss how to deal with duplicate points. Extended versions of the Algorithms with more sophisticated data structures and proper handling of boundaries and duplicates are then given in Section C.2 together with a bound on their worst-case complexity.

Preliminaries, induction strategy, cases 1 and 2. Throughout this proof we are simply going to write $c_{i,j}$ for $c(x_i,y_j)$. We assume that the point lists $\{x_i\}_{i=1}^n$ and $\{y_j\}_{j=1}^m$ are sorted, but we now allow for duplicate points and their handling will be addressed throughout this proof. Since c(x,y) = h(x-y) for h strictly convex, it is easy to verify that

$$c_{i,j} + c_{k,l} \le c_{i,l} + c_{k,j} \tag{15}$$

if $i \le k$ and $j \le l$, with a strict inequality if $x_i < x_k$ and $y_j < y_l$. This is known as Monge property [6]. The proof works via induction in the iterations of the main loop of Algorithm 1. We will show that prior to the iteration for x_k / after completing the iteration for x_{k-1} , the following holds:

- I. $\Psi_j \leq \lambda$ for all $j \in [1:m]$.
- II. For all $j \in [1:m]$, if $\Psi_j < \lambda$, then y_j is assigned.
- III. $\Phi_i \leq \lambda$ for all $i \in [1:n]$.
- IV. For all $i \in [1:k-1]$, if $\Phi_i < \lambda$, then x_i is currently assigned.
- V. All dual constraints $\Phi_i + \Psi_j \leq c_{i,j}$ for all $i \in [1:n], j \in [1:m]$ hold.
- VI. For all $i \in [1:n]$, $j \in [1:m]$, whenever x_i is assigned to y_j , one has $\Phi_i + \Psi_j = c_{i,j}$.
- VII. The assignment L will be monotonous. I.e. if $L[i] \neq -1$, $L[i'] \neq -1$ for i < i', then L[i] < L[i'].

We initialize with $\Psi_j = \lambda$ for all j, $\Phi_i = -\infty$ for all i, and empty assignment $L_i = -1$ for all i. Therefore, prior to the first iteration, when k = 0, all conditions are satisfied. Next, note that items (I) and (II) will be satisfied throughout the algorithm, since entries of Ψ are only ever decreased during the algorithm; entries are only decreased when the corresponding y_j are assigned; and once a point y_j is assigned, it may become re-assigned, but it never becomes un-assigned again. The claim that y_j is never un-assigned is clear in all cases apart from Case 3.1. In Case 3.1 it follows from property (VIII) below, which implies that when $x_{i_{\Delta}}$ is un-assigned from, say, $y_{j_{\Delta}}$, then $y_{j_{\Delta}}$ is re-assigned to $i_{\Delta}+1$ (since the assignment between $x_{i'}$ and $y_{j'}$ satisfies $L[i'] = j_{\min} + i' - i_{\min}$, i.e. the assignment is consecutive).

Throughout the algorithm let j_{last} be the largest index among any assigned points y_j . We initially set $j_{\text{last}} = -1$ when no y_j is assigned. Since assigned y_j do not get un-assigned (merely re-assigned), j_{last} is non-decreasing.

Lemma C.1. If $j_{\text{last}} \neq -1$, then during the iteration of the main loop of Algorithm 1, for any minimizer j^* in line 3 one has $y_{j^*} \geq y_{\text{last}}$. In particular, j^* can always be chosen such that $j^* \geq j_{\text{last}}$.

Proof. If $j_{\text{last}} = -1$ there is nothing to prove, since $j^* \geq 1$. If $j_{\text{last}} \neq -1$, then there must be some $i \in [1:k-1]$ such that $L[i] = j_{\text{last}}$ and therefore $\Phi_i + \Psi_{j_{\text{last}}} = c_{i,j_{\text{last}}}$. After adjusting Φ_k in line 4 one has $\Phi_k + \Psi_{j^*} = c_{k,j^*}$. By dual feasibility we have in addition

$$\Phi_k + \Psi_{j_{\text{last}}} \le c_{k,j_{\text{last}}},$$
 $\Phi_i + \Psi_{j^*} \le c_{i,j^*}.$

Combining these four (in-)equalities we get

$$c_{k,j^*} + c_{i,j_{\text{last}}} \leq c_{k,j_{\text{last}}} + c_{i,j^*}.$$

If $x_k > x_i$, then by (15) we have $y_{j^*} \ge y_{j_{\text{last}}}$. So $j^* < j_{\text{last}}$ can only happen if $y_{j^*} = y_{j_{\text{last}}}$ and thus we may also choose j_{last} as minimizing index. Therefore, we may impose the constraint $j^* \ge j_{\text{last}}$ in line 3. In the case $x_k = x_i$, assume j_{last} would not be a minimal index in line 3, i.e.

$$c_{k,j^*} - \Psi_{j^*} < c_{k,j_{\text{last}}} - \Psi_{j_{\text{last}}} = \Phi_i,$$

where in the last equality we used $x_k = x_i$. Since $L[i] = j_{\text{last}}$ one must have that the dual constraint for (i, j_{last}) must be active. This would imply that the dual constraint for (i, j^*) is violated, which contradicts the induction hypothesis.

Now during iteration k, the change of Φ_k in line 4, by construction, preserves (III) and (V). Assume we enter Case 1. The assignment function L is not changed, hence (VI) and (VII) remain preserved, and since $\Phi_k = \lambda$, (IV) is extended to i = k. Assume we enter Case 2. Then we have $L_k = j^*$, $\Phi_k + \Psi_{j^*} = c_{k,j^*}$ and $\Phi_k < \lambda$. Hence, (VI) remains true, and (IV) is extended to i = k. If we choose $j^* > j_{\text{last}}$ (which is possible by Lemma C.1), we preserve (VII).

Case 3. We now turn to Case 3.

Lemma C.2. In each iteration of the main loop of Algorithm 1, when we enter Case 3, i.e. $\Phi_k < \lambda$ and $j^* = j_{last}$, let i be the index such that x_i is currently assigned to $y_{j_{last}}$. Then $x_i = x_{i'}$ for all $i' \in [i:k-1]$. If i < k-1, then one must have $\Phi_i = \lambda$.

Proof. Clearly, i < k (since it was assigned during a previous iteration). In the following, let $f(x) = c(x, y_{j_{\text{last}}}) - \Psi_{j_{\text{last}}}$, which is convex in $x \in \mathbb{R}$. By (VI) we have $\Phi_i = c(x_i, y_{j_{\text{last}}}) - \Psi_{j_{\text{last}}} = f(x_i) \le \lambda$, by the current iteration of the main loop we have $\Phi_k + \Psi_{j_{\text{last}}} = c(x_k, y_{j_{\text{last}}}) = f(x_k) < \lambda$. Let now $i' \in [i+1, k-1]$. By monotonicity of L, (VII), if $L[i'] \ne -1$, then we would need $L[i'] > j_{\text{last}}$, which contradicts the definition of j_{last} . Therefore L[i'] = -1 and therefore by (IV) we must have $\Phi_{i'} = \lambda$. By (V) we must also have $\Phi_{i'} \le f(x_{i'})$, and by convexity of f, $f(x_{i'})$, since $f(x_i) \le \lambda$, $f(x_k) < \lambda$, this can only happen if $x_{i'} = x_i$, and $\Phi_i = f(x_i) = \lambda$.

This means that if all points are distinct, then we must have i = k - 1, and find ourselves in the main loop of Algorithm 2, see below.

Remark C.3. If points are not necessarily distinct (at least up to numerical rounding errors), and we find i < k - 1, then the situation can be remedied by setting L[i] = -1, $L[k] = j^*$, which preserves (VI), (IV) and (VII). We will add this to the algorithms in Section C.2.

We now study Algorithm 2 to resolve the conflict. In addition to the items above, at the beginning of each iteration of the main loop of Algorithm 2 the following is preserved:

VIII. There are indices
$$j_{\min} \leq j^*$$
, $i_{\min} \leq k-1$ with $j^* - j_{\min} = (k-1) - i_{\min}$ such that $L[i_{\min} + r] = j_{\min} + r$ for $r \in [0:(k-1) - i_{\min}]$, $\Phi_{i+r} + \Psi_{j_{\min}+r-1} = c_{i+r,j_{\min}+r-1}$ for $r \in [1:(k-1) - i_{\min}]$.

This is clearly true before the first iteration, when $i_{\min} = k - 1$ and $j_{\min} = j^*$. In each iteration of the main loop we then seek the largest possible value $\Delta \geq 0$ such that by setting $\Phi_i \leftarrow \Phi_i + \Delta$ for $i \in [i_{\min}, k]$ and $\Psi_j \leftarrow \Psi_j - \Delta$ for $j \in [j_{\min}, j^*]$ we preserve all items (I) to (VII). Clearly the delicate ones are (III) and (V). To preserve the former, we ensure that $\Delta \leq \lambda_{\Delta}$. To preserve the latter, we do not need to worry about the Ψ_j , $j \in [j_{\min}:j^*]$, since they are decreased, but we need to consider all constraints $\Phi_i + \Psi_j \leq c_{i,j}$ for $i \in [i_{\min}:k], j \in [1:j_{\min}-1] \cup [j^*+1:m]$. By the following lemma, we see that this can be reduced to checking the two constraints for $(i_{\min},j_{\min}-1)$ and (k,j^*+1) , which is the role of the variables α and β in Algorithm 2.

Lemma C.4. In the above situation, one has that

$$\begin{split} & \min_{i \in [i_{\min}:k], \atop j \in [j^*+1:m]} c_{i,j} - \Phi_i - \Psi_j = c_{k,j^*+1} - \Phi_k - \Psi_{j^*+1}, \\ & \min_{i \in [i_{\min}:k], \atop j \in [1:j_{\min}-1]} c_{i,j} - \Phi_i - \Psi_j = c_{i_{\min},j_{\min}-1} - \Phi_{i_{\min}} - \Psi_{j_{\min}-1}, \end{split}$$

if $j^* < m$ and $j_{\min} > 1$ respectively.

Proof. We start with the first equation and begin by showing that

$$c_{i,j} - \Phi_i - \Psi_j \ge c_{k,j} - \Phi_k - \Psi_j \tag{16}$$

for $i \in [i_{\min}:k], \ j \in [j^*+1:m]$. We get this by combining $\Phi_i \leq c_{i,j^*} - \Psi_{j^*}, \ \Psi_{j^*} = c_{k,j^*} - \Phi_k$ and the Monge property of cost matrix, (15), $c_{k,j} \leq c_{i,j} + c_{k,j^*} - c_{i,j^*}$. Next, observe that $\Psi_j = \lambda$ for $j \in [j^*+1:m]$, since these values have not yet been changed since the initialization, and $\Psi_{j^*} \leq \lambda$. Also we know that $\Phi_k = c_{k,j^*} - \psi_{j^*} \leq c_{k,j} - \psi_j$ for all $j \in [1:m]$. Combining this, we get $c_{k,j^*} \leq c_{k,j}$ for $j \in [j^*+1:m]$. Since $f: y \mapsto c(x_k, y)$ is convex, and $f(y_{j^*}) \leq f(y_j)$ for $j \geq j^*$, we must have that f is non-decreasing after y_{j^*} , and therefore among all indices $j \geq j^*$, the smallest one attains the minimum.

Now we turn to the second equation. In complete analogy to (16) we show that $c_{i,j} - \Phi_i - \Psi_j \ge c_{i_{\min},j} - \Phi_{i_{\min}} - \Psi_j$ for $i \in [i_{\min}:k], j \in [1:j_{\min}-1]$. Arguing as in Lemma C.1, we can show a minimizing index j can be chosen such that it is not smaller than \hat{j} , where \hat{j} is the largest index among the assigned y_j , that is less than j_{\min} (if such an assigned point exists, otherwise just let $\hat{j} = 0$ in the following). Consequently, all y_j points in $[\hat{j}+1:j_{\min}-1]$ must be unassigned and therefore have $\Psi_j = \lambda$. Arguing then via the convexity of c as in the previous paragraph, we can show that a minimizing j must be given by $j_{\min} - 1$.

The selection of Cases 3.1, 3.2 or 3.3 depends now on which of the three bounds λ_{Δ} , α , or β is smallest. Consequently, each of the implied updates of the dual variables in the three cases preserves the dual constraints and it is easy to see that by property (VIII) each of the conflict resolutions in Cases 3.1, 3.2 and 3.3a preserve all other conditions (I) to (VII). For instance, when λ_{Δ} is minimal, element $x_{i_{\Delta}}$ becomes unassigned, however we then have $\Phi_{i_{\Delta}} = \lambda$ as required by (IV).

We are left with discussing Case 3.3b, i.e. when β is minimal among the three bounds and $y_{j_{\min}-1}$ is already assigned. In complete analogy to Lemma C.2 we can prove the following.

Lemma C.5. In each iteration of the main loop of Algorithm 2, when we enter Case 3.3b, i.e. $\Phi_{i_{\min}} < \lambda$ and $y_{j_{\min}-1}$ is already assigned, let i be the index such that x_i is currently assigned to $y_{j_{\min}-1}$. Then $x_i = x_{i'}$ for all $i' \in [i:i_{\min}-1]$. If $i < i_{\min}-1$, then one must have $\Phi_i = \lambda$.

As above, this means that if all points are distinct, then $i=i_{\min}-1$, we can set $i_{\min}\leftarrow i_{\min}-1$, $j_{\min}\leftarrow j_{\min}-1$, note that we satisfy $\Phi_{i_{\min}}+\Psi_{j_{\min}}=c_{i_{\min},j_{\min}}$ and thus preserve (VIII) before the next iteration in Algorithm 2.

Remark C.6. If points are not all distinct and if $i < i_{\min} - 1$, then we must have $\Phi_i = \lambda$, thus we can unassign x_i and $y_{j_{\min}-1}$, and then proceed as if $y_{j_{\min}-1}$ were unassigned and resolve the conflict as in Case 3.3a.

C.2 Full algorithm versions and complexity

We now give more complete pseudo code versions of the Algorithms 1 and 2, see Algorithms 4 and 5. The main purpose is to reach a quadratic worst case time complexity. Our algorithm can be seen as a specialization of the Hungarian method, exploiting the particular one-dimensional structure of the cost and dealing consistently with the option to discard mass for a cost λ . The changes are explained below, subsequently some additional changes (for duplicate and boundary handling) are described in plain text, and finally we show how to determine the time complexity bound.

Algorithm 4: opt-1d

```
Input: \{x_i\}_{i=1}^n, \{y_j\}_{j=1}^m, \lambda
     Output: L, \Psi, \Phi
 1 Initialize \Phi_i \leftarrow -\infty for i \in [1:n], \Psi_i \leftarrow \lambda for j \in [1:m] and L_i \leftarrow -1 for i \in [1:n],
 \mathbf{2} \ j_{\text{last}} \leftarrow 1
 3 for k = 1, 2, ... n do
          j^* \leftarrow \operatorname{argmin}_{j \in [j_{\text{last}}:m]} c(x_k, y_j) - \Psi_j
 4
           \Phi_k \leftarrow \min\{c(x_k, y_{j^*}) - \Psi_{j^*}, \lambda\}
 5
 6
          if \Phi_k = \lambda then
              [Case 1] No update on L
 7
           else if j_{\min} - 1 unassigned then
 8
                [Case 2] L_k \leftarrow j^*, j_{\text{last}} \leftarrow j^*
 9
           else
10
                [Case 3] Run Algorithm 5.
11
```

Implemented modifications compared to Algorithms 1 and 2. Compared to Algorithm 1, in Algorithm 4 we have added the variable j_{last} for improved handling of duplicate points (or limited numerical precision), see Remark C.3. Note that initializing $j_{\text{last}} \leftarrow 1$, even when no points are yet assigned, yields the desired behavior. Additional adaptations related to this are discussed in the paragraph below.

Compared to Algorithm 2, there are several adaptations to Algorithm 5.

The dual variables Φ and Ψ are not updated during every loop of the algorithm but only once, when the conflict is resolved. This is handled via the auxiliary variable v and the auxiliary array d. The former stores the total increment that will need to be applied to Φ_k at the end, in addition d_i stores the value of v at the time when i was added to the 'chain', therefore $v-d_i$ will be the necessary increment of Φ_i at the end. This

```
Algorithm 5: sub-opt-full
```

```
Input: (\{x_i\}_{i=1}^n, \{y_j\}_{j=1}^m, k, j^*, j_{\text{last}}, L, \Phi, \Psi)
      Output: (Updated L, \Phi, \Psi, optimal for OPT(\{x_i\}_{i=1}^k, \{y_j\}_{j=1}^m), and j_{\text{last}})
  1 Initialize i_{\min} \leftarrow k - 1, j_{\min} \leftarrow j^*.
  2 Initialize v \leftarrow 0, d_j \leftarrow 0 for j \in [1:m], d_k \leftarrow 0, d_{k-1} \leftarrow 0.
  \mathbf{3} \ i_{\Delta} \leftarrow \operatorname{argmin}_{i \in [k-1:k]}(\lambda - \Phi_i), \ \lambda_{\Delta} \leftarrow \lambda - \Phi_{i_{\Delta}}
 4 while true do
             \alpha \leftarrow c(x_k, y_{j^*+1}) - \Phi_k - v - \Psi_{j^*+1}
  5
             \begin{split} \beta &\leftarrow c(x_{i_{\min}}, y_{j_{\min}-1}) - \Phi_{i_{\min}} - \Psi_{j_{\min}-1} \\ \text{if } \lambda_{\Delta} &\leq \min\{\alpha, \beta\} \text{ then} \end{split}
  6
  7
                     [Case 3.1]
  8
                    v \leftarrow v + \lambda_{\Delta}
  9
                     for i \in [i_{\min}, k-1] do
10
                      \Phi_i \leftarrow \Phi_i + v - d_i, \ \Psi_{L_i} \leftarrow \Psi_{L_i} - v + d_i
11
12
                     \Phi_k \leftarrow \Phi_k + v
13
                     L_{i_{\Delta}} \leftarrow -1, L_k \leftarrow j^*
                     for i \in [i_{\Delta} + 1 : k - 1] do
14
                      L_i \leftarrow L_i - 1
15
                   return
16
             else if \alpha \leq \min\{\lambda_{\Delta}, \beta\} then
17
                     [Case 3.2]
18
                     v \leftarrow v + \alpha
19
                     for i \in [i_{\min}, k-1] do
20
                      \Phi_i \leftarrow \Phi_i + v - d_i, \ \Psi_{L_i} \leftarrow \Psi_{L_i} - v + d_i
\mathbf{21}
                     \Phi_k \leftarrow \Phi_k + v
22
                     L_k \leftarrow j^* + 1, j_{\text{last}} \leftarrow j^* + 1
23
                 return
24
             else
25
                     v \leftarrow v + \beta
26
27
                    if j_{\min} - 1 unassigned then
                            [Case 3.3a]
28
                            for i \in [i_{\min}, k-1] do
29
                              \Phi_i \leftarrow \Phi_i + v - d_i, \ \Psi_{L_i} \leftarrow \Psi_{L_i} - v + d_i
30
                            \Phi_k \leftarrow \Phi_k + v
31
                            L_{i_{\min}} \leftarrow j_{\min} - 1, L_k \leftarrow j^*
32
                            for i \in [i_{\min} + 1 : k - 1] do
33
                              L_i \leftarrow L_i - 1
34
                           return
35
36
                     else
                            [Case 3.3b]
37
                            d_{i_{\min}-1} \leftarrow v, \, \lambda_{\Delta} \leftarrow \lambda_{\Delta} - \beta,
38
                            i_{\min} \leftarrow i_{\min} - 1, \, j_{\min} \leftarrow j_{\min} - 1
39
                            \begin{array}{l} \textbf{if} \ \lambda - \Phi_{i_{\min}} < \lambda_{\Delta} \ \textbf{then} \\ \ \  \  \, \bigsqcup \ \lambda_{\Delta} \leftarrow \lambda - \Phi_{i_{\min}}, \ i_{\Delta} \leftarrow i_{\min} \end{array}
40
41
```

trick (which is also known for the Hungarian method) removes the necessity to loop over the whole chain to update the dual variables during each iteration of the main loop in Algorithm 5 and thus reduces the worst case time complexity from cubic to quadratic.

Similarly, the index of the dual variable Φ_i that is currently closest to λ is not determined from scratch during each iteration. Instead, when case 3.3b is entered, the old best value is first reduced by β , then compared with the new competitor i_{\min} (after updating i_{\min}), and updated if necessary.

Additional recommended modifications to algorithm. In lines 5 and 6 of Algorithm 5 boundary checks should be added. E.g. α can only be set as described if $j^* < m$, otherwise it should be set to $+\infty$. Likewise, β can only be set as described if $j_{\min} > 1$ and should otherwise be set to $+\infty$. To keep track of which y_j are assigned one can use a boolean array of size m, initialized with false, and entries corresponding to assigned points are set to true. This can be used to distinguish between cases 3.3a and 3.3b. Alternatively, an 'inverse' version of L can be maintained, where $L^{-1}[j]$ will store the index i of point x_i to which point y_j is assigned (and -1 otherwise). This has to be updated consistently with L. The latter will be useful when dealing with duplicate points according to Remarks C.3 and C.6 at the beginnings of case 3 and case 3.3b, respectively.

Worst case time complexity. In Algorithm 4, initialization of the arrays Φ , Ψ and L requires $\Theta(n+m)$ steps. The main loop runs exactly n times. Determining j^* requires O(m) steps (using the particular structure of c and $\Psi_j = \lambda$ for $j > j^*$ one could reduce this further, see Lemma C.4, but we leave such optimizations for future work). Cases 1 and 2 take $\Theta(1)$ steps. Let us now consider case 3 and Algorithm 5. Initialization takes $\Theta(m)$ for setting up d (although we note that this initialization could be skipped). Cases 3.1, 3.2 and 3.3a are each entered only once, right before termination of the sub-routine, and they have a complexity of O(n) (iterating over the chain for a fixed number of times to adjust L and the duals). Case 3.3b, as well as maintaining the variables α , β and λ_{Δ} have a complexity of $\Theta(1)$ per iteration and there are O(n) iterations. Hence, Algorithm 5 in its current form has a complexity of $O(\max\{m,n\})$, and therefore finally Algorithm 4 has a complexity of $O(n \cdot \max\{m,n\})$. During the proof we have pointed out some potential for optimizing the algorithm for the regime when $n \ll m$.